REVIEWS OF TOPICAL PROBLEMS

New results for laser isotope separation using low-energy methods

Physics – Uspekhi **63** (3) 245 – 268 (2020)

REVIEWS OF TOPICAL PROBLEMS PACS numbers: 07.77.Gx, **33.80. – b, 36.40. – c, 42.62. – b**, 42.62.Fi, 82.40.Fp, 82.50.Bc

New results for laser isotope separation using low-energy methods

G N Makarov

DOI: https://doi.org/10.3367/UFNe.2019.02.038530

Contents

Abstract. Today, research aimed at the development of low-energy methods of molecular laser isotope separation (MLIS) is relevant and in demand. The main goal of these studies is to find efficient and cost-effective methods that can be used as the basis for the technology of laser separation of uranium isotopes, as well as other elements. To date, a number of approaches to the implementation of low-energy methods of MLIS using infrared (IR) lasers have been proposed. Many of these approaches are not well understood and/or are difficult to put into practice. Some of them are considered to be promising and require further study. These include the method of isotope-selective suppression of the clustering of molecules using IR lasers during gas-dynamic expansion at a nozzle exit and the method of isotope-selective IR dissociation of small molecular van der Waals clusters. A review of recent results obtained using these two methods is presented. The experimental facilities and research methods are briefly described, and the choice of the objects of study is substantiated. Results obtained with model SF_6 and CF_3Br molecules are analyzed with reference to studying the process of isotope-selective suppression of the clustering of molecules among themselves and with atoms of an argon carrier gas, as well as the process of isotope-selective IR dissociation of small homogeneous and mixed clusters of $(SF_6)_m Ar_n$ and $(CF_3Br)_m Ar_n$ (where $m = 1-2$ and $0 \leqslant n \leqslant 5$ are the numbers of molecules and atoms in the clusters, respectively). The results presented suggest that these methods can be used for the separation of isotopes in molecules containing isotopes of heavy elements, which have a slight isotopic shift in the IR absorption spectra.

Keywords: atoms, molecules, clusters, molecular and cluster beams, laser spectroscopy, laser-induced selective processes in molecules and clusters, laser separation of isotopes

G N Makarov Institute of Spectroscopy, Russian Academy of Sciences, ul. Fizicheskaya 5, 108840 Troitsk, Moscow, Russian Federation
E-mail: gmakarov@isan.troitsk.ru

Received 29 November 2018, revised 23 January 2019
Uspekhi Fizicheskikh Nauk **190** (3) 264 – 290 (2020)
Translated by Yu V Morozov; edited by V L Derbov

1. Introduction

Extensive research is currently underway aimed at the development of low-energy methods of molecular laser isotope separation (MLIS) [1–13]. The principal objective of these studies is the search for efficient and cost-effective techniques to separate isotopes of uranium and other elements. The application of the well-known method of selective infrared (IR) multiphoton dissociation (MFD) [14–17] that worked successfully when used to separate carbon

isotopes [18–21] proved inefficient for separating uranium isotopes because of high energy consumption, the lack of effective powerful laser systems, and a number of other factors [1]. Suffice it to say that around 40–45 quanta of IR radiation at a wavelength of 16 μm are needed to dissociate a single UF_6 molecule, which is equivalent to the absorption of 3.1–3.5 eV of energy per molecule.

One option for the further development of MLIS techniques is the use of low-energy physicochemical processes with an activation energy of no higher than 0.3–0.5 eV [1–13]. Such energies are inherent in the physicochemical processes of surface adsorption and desorption of molecules, including those on large cluster surfaces and in the processes of dissociation and fragmentation of weakly bound van der Waals molecules [1]. At present, the separation of isotopes by laser excitation (SILEX) technology for separating uranium isotopes is being developed in the USA [22–26]. The principles of this technology have not been disclosed, but there is reason to believe that it makes use of low-energy processes [27]. According to the developers of the SILEX technology, it can be applied to separate isotopes of other elements besides uranium, such as silicon, boron, sulfur, carbon, and oxygen [1, 22, 24].

To date, a large number of studies have been carried out devoted to low-energy MLIS using IR lasers [1–13], as well as alternative variants [28–31] (see references in review [1]). Many of these methods are not well understood and/or are difficult to put into practice. Some of them are considered to be promising and require further study. These include isotope-selective suppression of molecule clustering with the use of IR lasers during gas-dynamic expansion at a nozzle exit and isotope-selective IR dissociation of small molecular van der Waals clusters [1, 32–36]. The present review reports new results [37–44] obtained by these two techniques. The main interest in the described experiments and their results lies in the elucidation of the possibility of applying the methods under consideration for separating isotopes in molecules showing a slight isotopic shift in the IR absorption spectra as typical of UF_6 molecules. Therefore, the review is focused on this issue.

The paper is organized as follows. In Section 2 we consider the principles of methods for isotope-selective suppression of the clustering of molecules and isotope-selective IR dissociation of van der Waals clusters. The choice of the study objects is substantiated in Section 3. Section 4 describes the experimental setup and realization of the techniques for isotope-selective control of molecule clustering and isotope-selective dissociation of the clusters in concrete experiments. Sections 5 and 6 are devoted to the consideration and analysis of the data obtained in studies on isotope-selective suppression of the clustering of SF_6 and CF_3Br molecules among themselves and with argon atoms. Sections 7 and 8 present and discuss the results of selective IR dissociation of homogeneous and mixed van der Waals clusters $(SF_6)_m Ar_n$ and $(CF_3Br)_m Ar_n$, respectively. The concluding Section 9 summarizes the main results and the conclusions arising therefrom.

2. Principles of the methods

2.1 Isotope-selective suppression of the clustering of molecules

The method of isotope-selective suppression of molecule clustering in jets and flows using IR lasers [1, 32–36] is based on the preliminary (prior to clustering) vibrational excitation of the molecules, including those of a given type, during gas-dynamic expansion at the exit from the nozzle. The excitation causes the stored vibrational energy to suppress (prevent) clustering of excited molecules during subsequent condensation. Moreover, the proper choice of the place of particle irradiation at the jet axis in the space before the skimmer (Fig. 1) makes possible the dissociation of small clusters (dimers), which also can be used to control the molecule clustering process [37–44]. In this case, it is necessary to ensure preferential formation of the dimers in the absence of larger clusters, e.g., by the choice of suitable gas expansion conditions.

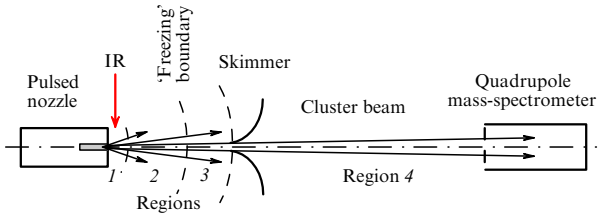

Figure 1. Formation of a cluster beam under pulse jet conditions. Numbers *1–4* schematically indicate regions differing in the degree of beam clustering [37, 41].

Today, this method is regarded as one of the possible and promising techniques for laser isotope separation [1–3, 6–8, 10, 12, 13]. The possibilities of its application to separate uranium isotopes were analyzed in Refs [7, 8]. The main characteristics of the method and related problems encountered in the operation of large-scale facilities for the separation of boron isotopes by the suppression of BCl_3 molecule clustering are discussed in recent publications [10, 12, 13]. To effectively realize the process on which the method of interest is based and ensure its high selectivity, a balance should be maintained precisely between the gas-dynamic jet cooling rate needed for cluster formation and the selective excitation of molecules of a given isotopic composition for the suppression of their clustering. The conditions necessary for controlled clustering are achieved by the choice of nozzle design and diameter, its operation regime (pulsed or continuous), gas composition, and temperature and pressure upstream of the nozzle. Equally essential are the spatial localization of the irradiation zone and parameters of IR radiation, such as wavelength and intensity. The choice of all these conditions depends on the individual characteristics of a concrete object [37–44].

An important issue in this context is the achievement of high product selectivity (or enrichment factors) necessitated by the relatively fast vibrational energy exchange between selectively excited and unexcited molecules due to the relatively high pressure near the nozzle. To decrease or prevent the rapid energy transfer between isotopomers, a strongly diluted mixture of molecules (less than 0.5–1%) with a carrier inert gas is usually used in experiments. The increased degree of dilution of molecules in an inert gas and the decreased total gas pressure upstream of the nozzle enhance isotope selectivity of the process [38–41]. The application of the method in question renders a cluster beam depleted of selectively excited molecules and enriched in unexcited ones, because free (unclustered) molecules are

distributed within a solid angle much broader than the cluster beam [45].

2.2 Isotope-selective IR dissociation of van der Waals clusters

The method of isotope-selective dissociation of weakly bound van der Waals molecules, in particular, dimers, for isotope separation is based on IR vibrational pre-dissociation of molecular clusters. At the early stages of the development of laser-assisted isotope separation techniques, the method was patented by Y T Lee [46], Nobel Laureate in Chemistry 1986, as a novel approach to separating isotopes of different elements. It was later studied by many authors [47–51]. Van der Waals molecules have one intramolecular bond weaker than the remaining ones, the difference between the binding energies being so great that vibrational quanta energies stored in the chemical bonds of their constituent monomer molecules exceeds the energy of dissociation of the weak van der Waals bond. As a result, such a molecule becomes metastable under vibrational excitation of a monomer and undergoes dissociation.

This property of van der Waals molecules is of great interest for the development of low-energy MLIS methods. For example, the bonding (dissociation) energy of polyatomic van der Waals molecules falls into the $0.1 \leqslant E_b \leqslant 0.5$ eV range, while the dissociation energy of van der Waals molecules composed of a polyatomic molecule and a noble gas atom $E_b \leqslant 0.1$ eV [52–56]. In other words, absorption of one or several quanta of IR radiation with a wavelength of about 10 μm, e.g., that of a CO_2 laser, leads to dissociation of their weak bond.

Spectroscopic studies of small molecular van der Waals complexes demonstrated [50, 52–55] that the absorption spectra of dimers and small clusters (either homogeneous or heterogeneous) are much narrower than those of free (unclustered) molecules; they have the form of narrow bands localized near vibrational frequencies of monomer molecules forming the clusters, making possible selective excitation and dissociation of the clusters (most frequently dimers) containing selected isotopomers and thereby facilitating isotope separation. In this method, cluster dissociation is accompanied by fragment (monomer) 'escape' from the beam. Thus, in a laboratory coordinate system target molecules (dissociation products) propagate within a relatively large solid angle determined by molecule mass and velocity, whereas non-target molecules stay in the near-axial part of the cluster beam. Experiments with the detection of molecular cluster beams by a mass-spectrometer reveal its depletion of excited (target) molecules.

3. Choice of the study objects

The authors of Refs [38–43] chose SF_6 [41, 42] and CF_3Br [38–40, 43] molecules as the study objects for the following reasons.

Both the structure and spectroscopic properties of the SF_6 molecule allow it to be regarded as a prototype of UF_6. It has been rather well explored both spectroscopically [57–61] and in terms of excitation and dissociation by IR laser radiation [14–17, 28–31]. Moreover, studies of IR absorption by small $(SF_6)_m$ ($m \leqslant 6$) clusters were undertaken near the absorption band of the laser-excited vibration ν_3 (948 cm^{-1}) of the molecule [62–64]. The low-resolution absorption spectra of small mixed complexes of $(SF_6)_mAr_n$ were obtained by the measurement of IR dissociations [34]. Also, the choice of this molecule was motivated by the necessity to estimate the possibility of improving selectivity in the processes of interest compared with those in earlier experiments [32–36].

The CF_3Br molecule was chosen for several reasons. First, it is characterized by a very small isotopic shift (≈ 0.248 cm^{-1} [65]) for $CF_3{}^{79}Br$ and $CF_3{}^{81}Br$ isotopomers in the spectrum of laser-excited vibration ν_1 (≈ 1085 cm^{-1} [65]). This gives rise to special interest in the study of the CF_3Br molecule in the context of applying the methods being considered for isotope separation in molecules with a slight isotopic shift in excited vibrations characteristic of molecules containing isotopes of heavy elements. For example, the isotopic shift for $^{235}UF_6$ and $^{238}UF_6$ isotopomers in the vibrational spectrum ν_3 (≈ 627 cm^{-1} [66]) is equally small (0.6 cm^{-1}) [66].

Second, many physical and chemical properties, as well as the type of symmetry of the CF_3Br molecule, are similar to those of CF_3I and its $(CF_3I)_m$ clusters, well studied in regard to IR multiphoton excitation of molecules [67, 68] and cluster fragmentation by IR and UV laser radiation [44, 69–74]. $(CF_3I)_m$ clusters are readily detectable due to the presence in their mass-spectrum of molecular and atomic ions (I_2^+ and I^+) formed during multiphoton cluster excitation by UV laser radiation [37, 69–71]. Similarly, CF_3Br molecules are equally well excited by CO_2 laser radiation [75, 76] and readily form clusters [38]. $(CF_3Br)_m$ clusters can also be detected by determining molecular ions Br_2^+ and atomic ions Br^+ (decay products of molecular ions) [38]. Reference [39] shows that $(CF_3Br)_m$ clusters can be detected by other ions of cluster fragments.

An important factor in the choice of CF_3Br molecules as a study object is the possibility of significantly simplifying the experimental conditions by taking advantage of the ratios of naturally occurring CF_3Br isotopomers. The comparable percentage content of $CF_3{}^{79}Br$ and $CF_3{}^{81}Br$ molecules in nature (50.56% and 49.44%, respectively) markedly facilitates mass-spectrometric detection of the isotopic ratio for bromine atoms as dissociation products of CF_3Br molecules and $(CF_3Br)_m$ and $(CF_3Br)_mAr_n$ clusters due to the presence of roughly equally strong Br^+ and Br_2^+ signals in the spectra of both isotopomers. The same is true of other signals of ions containing bromine atoms.

4. Experiment and implementation of the methods

4.1 Experimental facility

The experimental setup (Fig. 2) consists of a high-vacuum chamber with a pulsed source of a molecular cluster beam and a KMS-01/250 quadrupole mass-spectrometer (QMS). The upper bound of the range of detected mass numbers of the spectrometer $m/z = 300$ amu (z is the degree of ionization). The chambers of the molecular beam source and the mass-spectrometer were evacuated by turbomolecular pumps to a pressure of $\leqslant 10^{-5}$ and $\approx 10^{-7}$ Torr, respectively. The mass spectrometer was operated by a personal computer. A continuously frequency-tunable CO_2 laser was used in most cases to excite molecules and clusters in the jet. A pulsed CO_2 laser was used only in experiments on isotope-selective dissociation of mixed $(CF_3Br)_mAr_n$ clusters (see Section 8 below). The facility included in addition a pulse synchronizing system and a data collection/processing system.

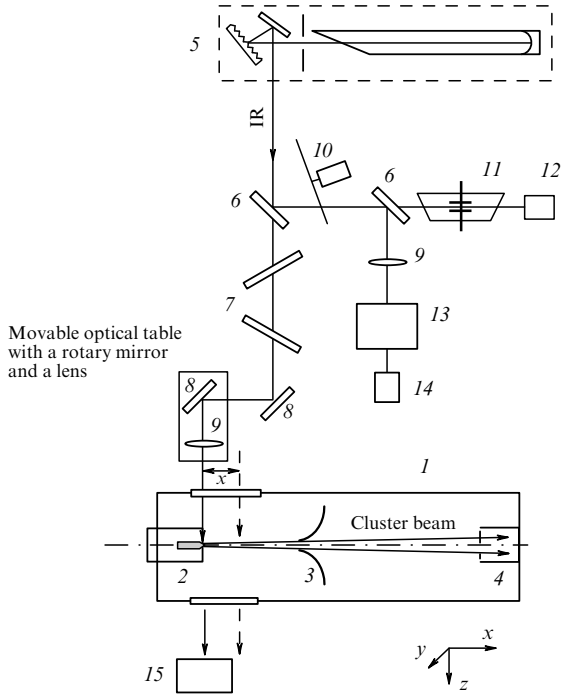

Figure 2. Layout of the experimental setup: *1* — vacuum chamber, *2* — pulsed nozzle, *3* — skimmer, *4* — quadrupole mass spectrometer, *5* — continuous-wave CO_2 laser, *6* — beam splitter, *7* — attenuators, *8* — flat mirror, *9* — lens, *10* — mechanical modulator, *11* — optoacoustic receiver, *12* — radiation detector, *13* — monochromator, *14* — radiation detector, *15* — power meter (movable) [39, 41].

The molecular cluster beam was generated in the source chamber by gas-dynamic cooling of the mixture of a gas of studied molecules with the carrier gas (mainly argon) as a result of supersonic expansion through a modified (see [37]) General Valve pulsed nozzle with an orifice diameter of 0.22 mm. Nozzles with orifice diameters of 0.16 or 0.25 mm were used in some experiments. The pulse repetition rate was 1 Hz. The half-height duration of the nozzle opening pulse varied from 0.3 to 1.6 ms, depending on the gas pressure and composition. Gas pressure upstream of the nozzle changed within a range of 1.3–5.0 atm. A skimmer (Beam Dynamics, Model 1) with an orifice diameter of 0.49 mm placed 35 mm from the nozzle cut out a molecular cluster beam from the central part of the supersonic flow created by the nozzle. The beam thus formed entered the ionization chamber of the quadrupole mass-spectrometer. The distance between the nozzle and the spectrometer chamber was 570 or 250 mm.

The continuous-wave CO_2 laser used in the experiments had a semi-confocal resonator. The laser power amounted to 13 W. Its IR radiation was introduced into the molecular cluster beam chamber through a window by means of copper mirrors and a spherical lens with the focal length $f = 200$ mm (see Fig. 2). The diameter of the IR radiation spot in the lens focus was ≈ 0.5 mm. The laser beam crossed the molecular-cluster beam at an angle of 90° and could be moved along its axis with the help of a movable table. The laser radiation power was altered with the use of attenuators. IR radiation that passed through the chamber was measured by a power meter. CO_2 laser tuning to the selected generation lines was monitored using an optoacoustic receiver filled with ammonia. The ammonia IR absorption lines served as the benchmarks for laser frequency tuning.

4.2 Implementation of the methods

The process of gas clustering during gas-dynamic expansion at the exit from the nozzle can be divided into the following several stages (see Fig. 1) that occur in different regions of the jet [37–42]: *1* — the region of rapid cooling of translational and internal degrees of freedom of molecules with an energy transfer to the kinetic energy of the directed flow movement and medium transition to the oversaturated state with the formation of seed clusters; *2* — the collision region where gas-dynamic cooling of molecules continues in parallel with the growth of clusters in the jet and some heating of the system due to the condensation energy; *3* — the region beyond the 'freezing' boundary, i.e., transition to the collisionless movement of the particles and cluster system stabilization; *4* — the region between the skimmer and the mass spectrometer where the free flight of beam particles takes place.

To study the influence of resonant IR excitation of jet molecules on cluster beam formation at different clustering stages, it is necessary to irradiate particles in the respective jet regions at the trajectory of the flow forming the cluster beam and register changes in beam parameters in the detection zone. Weakening of the signal from the cluster constituent of the beam may be due to several factors [37–42].

If a jet is irradiated in region *1*, IR excitation of the molecules leads to a local rise in temperature, which hampers nucleation. Ideally, this can prevent further molecule clustering. If molecules are strongly diluted with an inert gas, the probability of their collision is low, and selective suppression of the clustering of excited molecules is possible.

IR laser irradiation of particles in region *2* causes vibrational heating of the molecules and clusters formed in the jet at this point. Simultaneously, some of the clusters are likely to undergo fragmentation. Heating of the particles occurs against the background of their competing gas-dynamic cooling (especially in the presence of a carrier gas) and some further change in the jet cluster composition (growth of clusters, evolution of their size distribution).

If particles are irradiated in region *3* (in the absence of collisions), the action of IR radiation reduces largely to cluster heating and fragmentation manifested as a weakening of the signal from the cluster constituent of the beam.

It can be concluded that excitation of jet particles in regions *1–3* by resonant IR laser radiation can either suppress molecule clustering or cause dissociation of the newly formed clusters, depending on the location of the concrete irradiated area [37–44].

To recall, the physical nature of the observed processes in such experiments changes significantly as a function of the position of the irradiated site with respect to the nozzle exit section. Excitation of molecules near the nozzle exit section eventually suppresses molecule clustering and reduces the strength of the observed clustering signal. If the molecules are excited rather far from the nozzle, cluster dissociation predominates (see Sections 7 and 8) and weakening of the cluster signal is caused by IR vibrational pre-dissociation of the clusters. Transition from one process to the other determines the behavior of the cluster signal measured in the experiment [37–44] (see Sections 5–8).

It should be noted that both the strength and the character of ion signals from molecules and clusters depend on the electron energy in the mass-spectrometer ionizer, as well as on the internal energy of the particles undergoing ionization. The electron energy in different experiments ranged from 40 to 70 eV. However, it remained constant in each concrete

experiment. We did not observe in our experiments any appreciable change in signal ratios for different isotopic components attributable to electron energy variation within the aforementioned range [38–43]. A change in electron energy affected only the strength of ion signals. Nor could we document a marked (around 1–2%) alteration in the ion signal ratio for vibrationally excited and unexcited molecules and clusters. This probably accounts for the rather small internal energy of the particles excited by low-intensity laser radiation in experiments [38–43].

5. Isotope-selective suppression of the clustering of SF_6 molecules

5.1 Selective suppression of the clustering of SF_6 molecules among themselves

5.1.1 Details of the experiment and relevant remarks. Selective suppression of the clustering of SF_6 molecules among themselves was the subject of a thorough investigation in Ref. [41]. Its main objective was to elucidate the conditions under which resonant vibrational excitation of molecules markedly affects $(SF_6)_m$ cluster nucleation and growth in a gas-dynamic jet and to determine the dependences of the efficiency and selectivity of the suppression of molecule clustering on gas composition and pressure upstream of the nozzle and on laser radiation parameters. In addition, the experiments reported in Ref. [41] included the search for the optimal conditions under which isotope-selective suppression of molecule clustering is maximally efficient.

Pulsed nozzles with an orifice diameter of 0.16 or 0.25 mm were used in Ref. [41]. The length of the nozzle opening pulse varied from 1 to 1.2 ms, depending on the gas pressure and composition upstream of the nozzle. The gas pressure upstream of the nozzle changed within a range of 1.3–3.0 atm. The distance between the nozzle and the spectrometer chamber was 570 mm. A lens with focal distance $f = 110$ mm was used to focus laser radiation onto the area of intersection with the jet axis; the laser beam diameter at the 1/e level was 0.58 mm and the half-height diameter 0.49 mm. The experiment was designed to measure and compare ion signals from cluster and molecule constituents of the beam without particle excitation and after the excitation of beam molecules and clusters by laser radiation.

The method for estimating selectivity α of the laser control over molecule clustering was as follows. Selectivity was determined from the results of the measurement of ion signals from SF_5Ar^+, $SF_6SF_5^+$ cluster fragments and the SF_5^+ ion signal, to which an appreciable contribution comes from cluster fragmentation. Also measured in the experiment was the fractional contribution $q = (q_1, q_2, q_3)$ to the registered ion signal from each of the three sulfur isotopes, ^{32}S, ^{33}S, and ^{34}S, relative to its initial natural content. The measured mass spectra were fitted by a Gaussian function; thereafter, q values were found. Selectivity in the case of excitation of the ith isotopomer of SF_6 molecules with respect to the jth isotopomer was defined as $\alpha(i/j) = (1 - q_j)/(1 - q_i)$. Such a definition suggests the statistically determined formation of various isotopic modifications of the clusters, e.g., dimers. Since the concentration of ^{33}S was relatively low (0.75%), all calculations were made for ^{32}S and ^{34}S isotopes.

Figure 3 illustrates the dependence of the relative strength of the S_{IR}/S_0 cluster signal (laser on/laser off) on the distance between the particle irradiation zone (the laser spot) and the nozzle exit. Also shown are the nozzle head position and the size of the laser spot. The 273-amu ion peak corresponding to the $^{32}SF_6{}^{32}SF_5^+$ ion fragment of the $(SF_6)_2$ dimer is taken as the cluster signal.

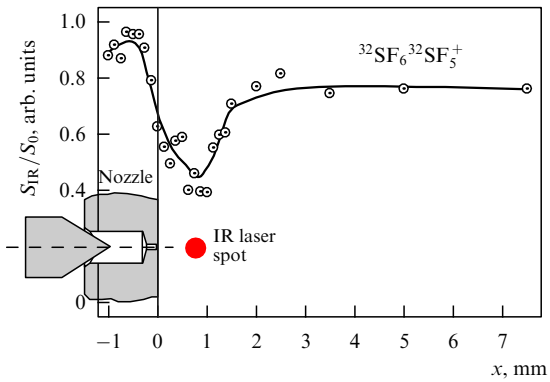

Figure 3. Relative value of cluster signal S_{IR}/S_0 versus laser beam position (nozzle exit section and laser spot size are depicted to scale). The jet was irradiated by the 10P(14) CO_2 laser line (frequency 949.48 cm^{-1}). Radiation power in the chamber was 9 W. An SF_6/Ar gas mixture with the pressure ratio of 1/100 and total pressure 1.33 atm was used upstream of the nozzle. Nozzle opening pulse length: 1 ms (at half-height) [41, 42].

The dependence shows a clearly apparent dip in the case of jet irradiation near the nozzle exit section. The minimal value of the signal at this line is $\sim 40\%$ of the initial one (without excitation). It partly recovers up to $\sim 80\%$ as the distance from the nozzle increases but remains unaltered thereafter. The dip is roughly 1.4 mm wide (an equivalent to 5–6 nozzle calibers). The signal in the negative displacement region corresponds to laser beam contact with the nozzle edge, while the dip corresponds to the area in which clustering of SF_6 molecules is suppressed as a result of their vibrational excitation. An increase in the distance between the nozzle and the particle irradiation zone leads to a transition into the area of advanced and 'frozen' condensation; therefore, the decrease in the signal in this region is largely due to cluster dissociation by IR laser radiation [36, 37, 44, 77] (see Sections 7, 8).

Most measurements in experiments with a mixture of SF_6 molecular gas and argon were made for an SF_6/Ar mixture at a pressure ratio of 1/200. It was shown in [41] that selective suppression of the clustering of SF_6 molecules among themselves and with argon atoms took place under these conditions. Selectivity worsened significantly at a low dilution, whereas a higher dilution was associated with a decrease in the signal-to-noise ratio, which hampered measurements.

5.1.2 Dependence of molecular clustering suppression on laser frequency. Changes in the intensity of the beam cluster constituent induced by IR excitation of the respective isotopic component of the SF_6 molecule were determined by monitoring the behavior of (decrease in) the signals from $SF_6SF_5^+$, $ArSF_5^+$, SF_5^+ ion products and their isotopic composition. Figure 4a presents the dependence of the strength of the $^{32}SF_6{}^{32}SF_5^+$ dimer ion signal on the distance between the particle irradiation zone and the nozzle exit (the size of the laser beam cross section in the focus is shown below). Measurements were made with the use of two CO_2 laser generation lines, 10P(16) (frequency 947.74 cm^{-1}) and 10P(34) (frequency 931.00 cm^{-1}), to excite jet particles. The former line is in resonance with $^{32}SF_6$ molecules [60], the latter

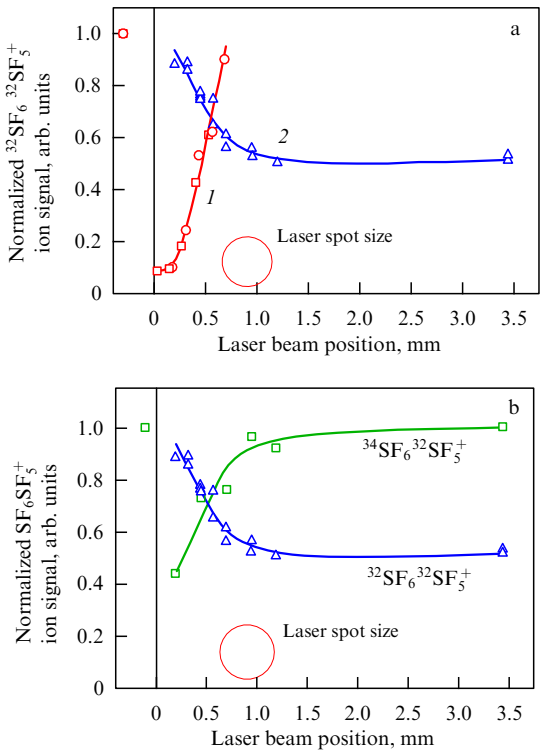

Figure 4. (a) Dependences of normalized $^{32}SF_6{}^{32}SF_5^+$ ion signal on the distance between the nozzle exit and the particle irradiation zone with excitation at different laser lines (frequencies). Curve *1*: the 10P(16) line (947.74 cm^{-1}), laser power is 4.1 W. Curve *2*: 10P(34) line (931.00 cm^{-1}), laser power is 5.8 W. (b) Dependences of normalized $^{34}SF_6{}^{32}SF_5^+$ and $^{32}SF_6{}^{32}SF_5^+$ ion signals on the distance between the nozzle exit and the particle irradiation zone with excitation at the 10P(34) line; laser power is 5.8 W. SF_6/Ar gas mixture with pressure ratio 1/200 and total pressure 2 atm was used upstream of the nozzle. Nozzle opening pulse length was 1.2 ms [41].

with $^{34}SF_6$ [61]. The behavior of the measured curves is significantly different. In the first case, with the laser beam being close to the nozzle exit (where the impact of laser radiation on free molecules is still possible), the $^{32}SF_6{}^{32}SF_5^+$ dimer signal is almost fully suppressed.

As the laser beam moves away from the nozzle exit, the signal is restored practically up to the initial level (experimental points are two series of independent measurements). The most pronounced decrease in the cluster signal is associated with the resonant excitation of molecules near the nozzle exit section where they are still free and clusters do not form. Molecule condensation begins at a distance from the nozzle where the spectrum of the newly formed particles goes off resonance with laser radiation and the dimer signal recovers. $(SF_6)_2$ dimers practically do not absorb IR laser radiation at the 10P(16) line. A similar dependence of the ion signal on the distance between the nozzle and the absorption zone in the case of excitation at the 10P(16) line is documented for other ion products, e.g., $ArSF_5^+$ and SF_5^+ [41].

A different picture is observed when particles are excited at line 10P(34) and laser radiation is in resonance with $^{34}SF_6$ molecules [61]. However, the excitation of this isotopic component near the nozzle exit in the experiments being considered hardly affects the $^{32}SF_6{}^{32}SF_5^+$ signal due to the selectivity of the process. At the same time, line 10P(34) falls into the $^{32}SF_6{}^{32}SF_6$ absorption band [63]. Therefore, the decrease in the respective ion signal should be attributed to dissociation of the dimers that form in increasing numbers as distance between the particle excitation region and the nozzle increases. The onset of saturation of the $^{32}SF_6{}^{32}SF_5^+$ signal is probably due to the insufficient laser radiation power and the contribution from larger clusters.

The dependence on the distance between the nozzle and the irradiation zone for an ion signal with a different isotopic modification, such as $^{34}SF_6{}^{32}SF_5^+$, excited at line 10P(34), essentially differs from the dependence for $^{32}SF_6{}^{32}SF_5^+$. It is clearly demonstrated in Fig. 4b (cf. the upper and lower curves). In this case, laser radiation excites $^{34}SF_6$ molecules, and particle irradiation near the nozzle exit suppresses formation of $^{34}SF_6{}^{32}SF_6$ dimers.

Importantly, the characteristic spatial size of the 'dip' (Fig. 4a) for all products amounts to 0.4–0.5 mm, i.e., it is roughly equal to the laser beam diameter. This means that the length of the region in which molecule clustering is most effectively suppressed does not exceed 2–3 nozzle calibers.

5.1.3 Dependence of molecular clustering suppression on laser power. The dependence of the efficacy of SF_6 molecule suppression on laser radiation power was evaluated based on measurements of ion signals from $ArSF_5^+$, SF_5^+, and $SF_6SF_5^+$ fragments. The results obtained for $ArSF_5^+$ and SF_5^+ cluster ions are presented in Fig. 5a.

SF_5^+ ion signals were measured when particles were irradiated at three different distances from the nozzle. The practically exponential decrease in the SF_5^+ signal was observed with its subsequent saturation. The solid lines in Fig. 5a are the result of approximation of experimental data by the function $f(W) = C_1 + (1 - C_1)\exp(-W/W_0)$, where W is the laser power, and C_1 and W_0 are the fitting parameters. The most considerable reduction in the signal occurs at the smallest distance of the laser beam from the nozzle. $ArSF_5^+$ ions display a similar behavior, but the fall of their signals is even more pronounced. Notably, the ion signals tend to be saturated. It is difficult to unambiguously explain such behavior of the curves for the $ArSF_5^+$ signal, because the primary source of these ions remains unknown. It can be speculated that the signal receives a contribution from the ionization of mixed clusters of a different size.

A more consistent explanation is offered for a similar dependence for $SF_6SF_5^+$ ions, illustrated by Fig. 5b. The main contribution to this signal in the SF_6 gas strongly diluted in argon comes from $(SF_6)_2$ dimer dissociation due to the low probability of large cluster formation under these conditions [78]. Fig. 5b presents separately the dependences of $^{32}SF_6{}^{32}SF_5^+$ and $^{34}SF_6{}^{32}SF_5^+$ ion signals on the laser power. Clearly, a high enough radiation power makes possible practically complete suppression of the $^{32}SF_6{}^{32}SF_5^+$ signal and a somewhat slighter suppression of the $^{34}SF_6{}^{32}SF_5^+$ signal.

The observed difference in the behavior of the dependences of the signals from various ion clusters on the laser radiation power clearly demonstrates isotopic selectivity of molecule clustering suppression. In particular, it follows from the data on relative isotope concentrations in dimers that selectivity at a laser power of 4 W can be estimated as $\alpha(^{32}S/^{34}S) \approx 3.5$.

5.1.4 Suppression of the clustering of SF_6 molecules among themselves. An important characteristic of the process under study is the dependence of selectivity of SF_6 clustering suppression on the power of laser radiation exciting the

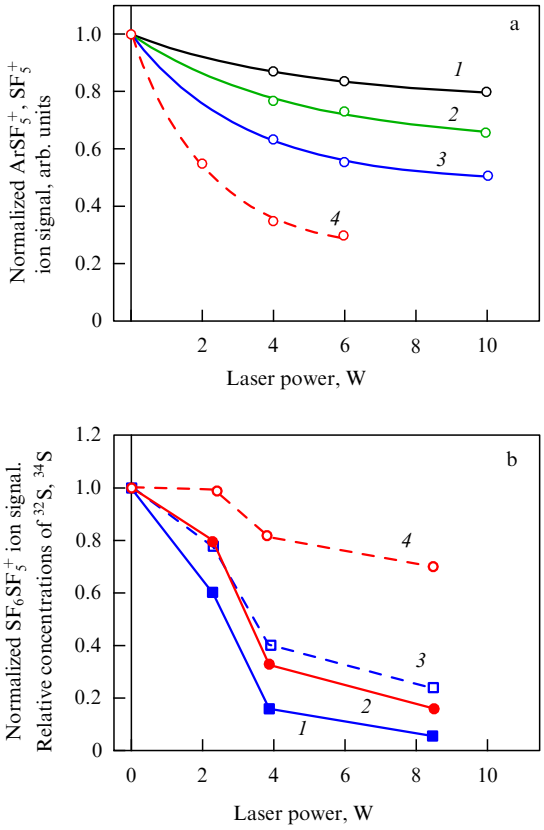

Figure 5. (a) Dependences of normalized SF_5^+ (curves *1–3*) and $ArSF_5^+$ (curve *4*) ion signals on laser power for particle excitation at line 10P(16) (947.74 cm^{-1}). Circles indicate experimental points, smooth curves are approximations (see the text). SF_5^+ ion signal was measured at different distances from the nozzle: 0 mm (curve *1*), with laser beam touching the nozzle, 0.25 mm (curve *2*), and 0.5 mm (curve *3*). (b) Dependences of normalized $SF_6SF_5^+$ ion signal and relative concentrations of ^{32}S and ^{34}S isotopes on laser power. Curve *1* — $^{32}SF_6{}^{32}SF_5^+$ ion signal, curve *2* — $^{34}SF_6{}^{32}SF_5^+$ ion signal. Curves *3* and *4* — relative concentrations of ^{32}S and ^{34}S isotopes, respectively. Laser generation line is 10P(16). A mixture of SF_6/Ar gases with pressure ratio of 1/200 and total pressure 2 atm was used upstream of the nozzle. Nozzle pulse duration is 1.2 ms [41].

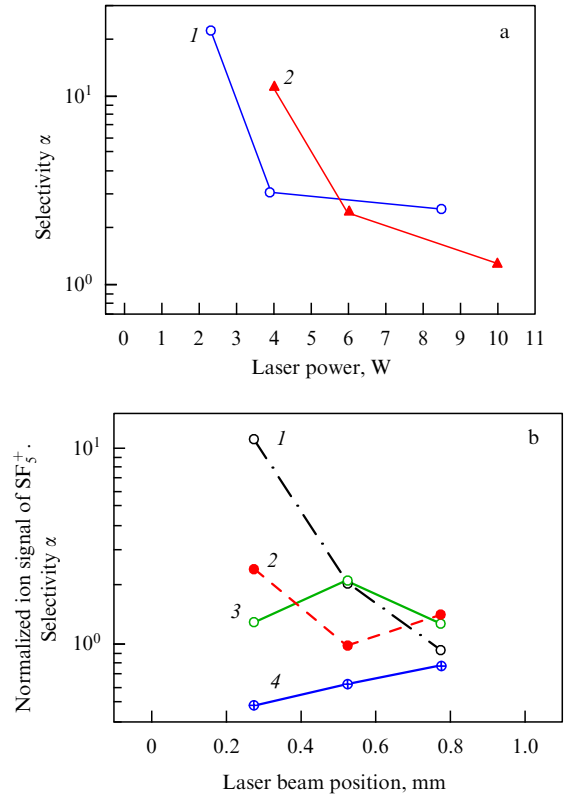

Figure 6. (a) Dependences of selectivity of SF_6 clustering suppression on laser power measured by $SF_6SF_5^+$ and SF_5^+ cluster ion signals (curves *1* and *2*, respectively). Laser generation line 10P(16). A mixture of SF_6/Ar gases with pressure ratio of 1/200 and total pressure 2 atm was used upstream of the nozzle. Duration of the nozzle pulse is 1.2 ms [41]. (b) The dependences of selectivity of SF_6 clustering suppression on the distance between the particle irradiation zone and the nozzle exit measured by SF_5^+ cluster ion signals. Curves *1*, *2*, and *3* were obtained at a laser power of 4, 6, and 10 W. Curve *4* is normalized SF_5^+ ion signal. The laser generation line and gas expansion conditions are the same as in Fig. 6a [41].

particles. Characteristic dependences of parameter α on the power of a CO_2 laser determined from $SF_6SF_5^+$ and SF_5^+ ion signals during particle excitation at the 10P(16) line with preferential suppression of $^{32}SF_6$ clustering are presented in Fig. 6a. Despite the relatively small number of experimental points, Fig. 6a clearly demonstrates that selectivity progressively decreases with increasing laser radiation power. It is worthy of note that rather high selectivity $\alpha \approx 20$ was achieved at a relatively low laser power of ≈ 2 W [41].

Reference [41] reports the measurement of the dependence of SF_6 clustering suppression selectivity on the distance between the particle irradiation zone and the nozzle at different laser power values. Results of the measurement for SF_5^+ ions are presented in Fig. 6b. Evidently, selectivity decreases at all laser power values as the distance between the irradiation zone and the nozzle increases. A similar distance dependence of selectivity observed for the $SF_6SF_5^+$ dimer ion is illustrated in Fig. 7.

Moreover, at large enough distances from the nozzle, where the radiation enters the region occupied largely by clusters, the selectivity changes by $\alpha < 1$ (Fig. 7). This may be due to selective dissociation of the clusters containing $^{34}SF_6$ molecules. In this region, the $^{32}SF_6{}^{32}SF_5^+$ signal fully recovers, while the $^{34}SF_6{}^{32}SF_5^+$ signal slightly drops, which accounts for the change in selectivity. To recall, calculations in [63] show that one of the $^{32}SF_6{}^{34}SF_6$ dimer absorption peaks is located near the 10P(16) frequency of the laser line.

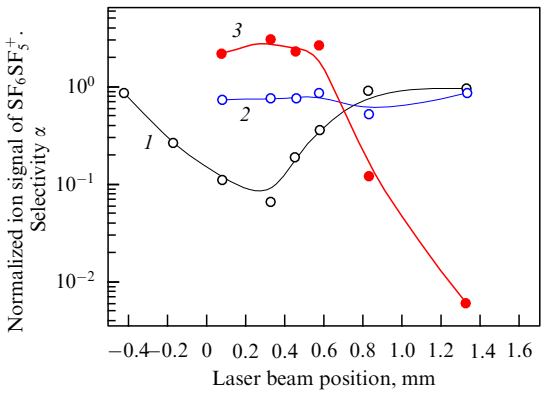

Figure 7. Dependence of selectivity of SF_6 clustering suppression (curve *3*) on distance between particle irradiation zone and nozzle exit measured by $SF_6SF_5^+$ ion signals. Curves *1* and *2* are $^{32}SF_6{}^{32}SF_5^+$ and $^{34}SF_6{}^{32}SF_5^+$ ion signals, respectively. Laser generation line is 10P(16), radiation power is 6 W. A mixture of SF_6/Ar gases at pressure ratio of 1/200 and total pressure 2.4 atm was used upstream of the nozzle. Duration of the nozzle pulse was 0.3 ms [41].

Table 1. Some results on selectivity of suppression of SF_6 molecule clustering among themselves and with argon atoms (highlighted in bold) during gas-dynamic expansion of an SF_6/Ar mixture under different experimental conditions. The particles were irradiated at the laser 10P(16) line (frequency 947.74 cm^{-1}). Total gas pressure upstream of the nozzle: 2 atm [41].

Gas composition upstream of the nozzle	Laser power, W	Selectivity of suppression of the clustering of SF_6 molecules among themselves $\alpha(^{32,32}S/^{34,32}S)$	Selectivity of suppression of the clustering of SF_6 molecules with argon atoms $\alpha(^{32}S/^{34}S)$	Duration of a nozzle pulse, ms	Distance x from the particle irradiation zone to the nozzle, mm
$SF_6/Ar = 1/200$	4	≈ 3.5		1.2	0.5
$SF_6/Ar = 1/200$	2	≈ 20		1.2	0.25
$SF_6/Ar/CH_4 = 1/195/4$	4	$\geqslant 15$		1.2	0.1
$SF_6/Ar = 1/200$	**7.2**		**$\geqslant 25-30$**	**1.6**	**1.25**

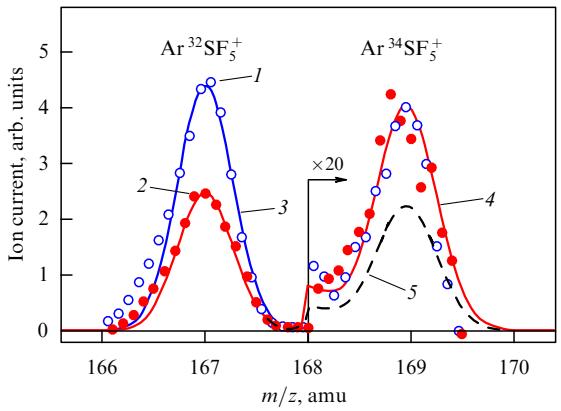

Figure 8. Ar $^{32}SF_5^+$ and Ar $^{34}SF_5^+$ ion peaks: initial signal without IR irradiation (curve *1*) and after IR irradiation at the 10P(16) line (curve *2*). Smooth curves *3*, *4*, and *5* are model signals for $ArSF_5^+$ ions containing ^{32}S, ^{33}S, and ^{34}S isotopes in relative concentrations $q(^{32}S, ^{33}S, ^{34}S)$ equal to (1, 1, 1), (0.56, 1, 1), and (0.56, 0.56, 0.56), respectively. (1, 1, 1) stands for the natural isotope ratio. The laser is tuned to line 10P(16), its power is 7.2 W. A mixture of SF_6/Ar gases with the pressure ratio 1/200 and total pressure 2 atm was used upstream of the nozzle. Duration of the nozzle pulse was 1.6 ms [41].

5.2 Selective suppression of the clustering of SF_6 molecules with argon atoms

Selectivity of the suppression of the clustering of SF_6 molecules with argon atoms was studied in [41] using mixed $(SF_6)_m Ar_n$ clusters and measuring SF_5Ar^+ ion peaks. An SF_6/Ar mixture was used at a pressure ratio of 1/200 and total gas pressure upstream of the nozzle 2 atm. The jet was irradiated at the laser 10P(16) line (947.74 cm^{-1}) 1.25 mm from the nozzle. This generation line was in resonance with $^{32}SF_6$ molecules [60]. The results are presented in Fig. 8, showing the strength of $^{32}SF_5Ar^+$ and $^{34}SF_5Ar^+$ ion signals without and with irradiation of the jet. Curves *4* and *5* in Fig. 8 indicate signal values calculated taking into account the ratio of sulfur isotopes normalized to their natural content.

Figure 8 shows that the best agreement between calculated and experimental ratios of isotopomers was obtained for $q = (0.56, 1, 1)$, i.e., when the $^{34}SF_5Ar^+$ peak does not decrease at all, which formally corresponds to 'infinite' selectivity. Thus, in the considered work [41] the control of SF_6 clustering with argon atoms ensured a very high degree of selectivity $\alpha(^{32}SF_6/^{34}SF_6) \geqslant 25-30$ (see also Table 1).

5.3 Results of studies with other carrier gases

One of the important consequences of using the SF_6/Ar mixture is the small size of the spatial region in which selective suppression of molecule clustering may occur; it does not exceed 2–3 nozzle calibers. The use of other carrier gases makes it possible to vary the relaxation rate and thermal capacity of the expanding gas if we use molecular gases for this purpose. It allows, in principle, controling the heat capacity and relaxation rate of the system by changing both gas pressure and composition upstream of the nozzle and thereby altering the length of the region of cooling and subsequent condensation of the molecules, as well as parameters of laser-assisted suppression of clustering.

Reference [41] reports experiments with the use of helium, krypton, methane, and their mixtures with argon as carrier gases. The choice of methane was motivated by its high thermal capacity due to the presence of vibrational and rotational degrees of freedom. Moreover, a small addition of methane to noble gases is known to have been used to suppress cluster formation in experiments with UF_6 [79]. In all these studies [41], the degree of SF_6 dilution compared with that of other mixture components remained at the same level ($\approx 1/200$) at which experiments with argon as the carrier gas were carried out.

It should be emphasized that no appreciable improvement in selectivity was reached when other gasses were used as carriers instead of argon [41]. One of the results closest to that in Ref. [41] was obtained using $SF_6/Ar/CH_4 = 1/195/4$ (Fig. 9a) (see also Table 1). The dependences of $^{32}SF_6{}^{32}SF_5^+$ and $^{34}SF_6{}^{32}SF_5^+$ signals on the distance between the particle irradiation zone and the nozzle are analogous to those obtained earlier for carrier argon. The distance dependence of selectivity behaves similarly (Fig. 9b). When the irradiation area lies 0.5 mm from the nozzle, selectivity equals unity. At smaller distances, it is higher, and at larger ones, it is lower than that.

At the same time, in Ref. [41] it was found that a change in the carrier gas composition alters the composition of ion products in the mass spectrum and the efficacy of SF_6 cluster formation. The length of the region in which selective control of clustering is possible proved roughly equal (with an accuracy up to the measurement error) for all the mixtures used. A slight enlargement of this region was observed only in the case of a high dilution of the study SF_6 gas by adding methane, e.g., for $SF_6/Ar/CH_4 = 1/50/150$, probably because of the enhanced heat capacity of the gaseous system and the resulting increase in its relaxation and cooling times.

5.4 Selected estimates and conclusions

Here are some estimates allowing a better understanding of the relationship among parameters of the process under study [41]. The estimates are based on data on the width and the shape of the IR absorption spectra of SF_6 isotopomers at low temperature (around 50 K) [80] and a small ($\leqslant 100-150$ MHz) width of the CO_2 laser radiation spectrum. Taking account of these parameters allows concluding that the optical selectivity of $^{32}SF_6$ molecule excitation relative to $^{34}SF_6$ at a frequency of 947.74 cm^{-1} on the

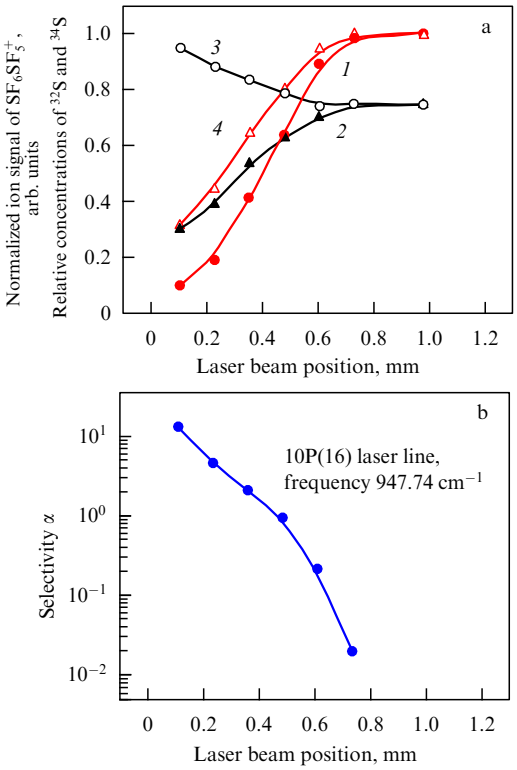

Figure 9. (a) Normalized $^{32}SF_6{}^{32}SF_5^+$ and $^{34}SF_6{}^{32}SF_5^+$ ion signals (curves *1* and *2*, respectively) and relative concentrations of ^{34}S and ^{32}S isotopes (curves *3* and *4*) versus distance between particle irradiation zone and nozzle exit for $SF_6/Ar/CH_4 = 1/195/4$ upstream of the nozzle. (b) Selectivities of molecule clustering suppression. The laser is tuned to line 10P(16), its power is 4 W. A mixture of $SF_6/Ar/CH_4$ gases with the pressure ratio of 1/195/4 and total pressure 2 atm was used upstream of the nozzle. Duration of the nozzle pulse: 1.2 ms [41].

10P(16) laser line is $\alpha_{exc}(^{32}S/^{34}S) > 10^2$. Selectivities of suppression of the molecule clustering observed in [41] are much lower than that.

We believe that the impairment of selectivity is caused by the following factors. First, the effective vibrational energy exchange between $^{32}SF_6$ and $^{34}SF_6$ molecules may be the principal factor responsible for the loss of selectivity in the process of control over molecule clustering. Second, the jet in the zone of molecule excitation near the nozzle exit is not yet sufficiently cold and the particle temperature is therefore much higher than 50 K. Due to this, optical selectivity of the excitation is lower than the above value. Moreover, a rather large size of the laser spot (≈ 0.5 mm in diameter) makes the particle irradiation region much greater than the region of maximum selectivity of excitation in terms of molecule concentration and temperature. In a jet rapidly expanding in space and time, these parameters strongly vary, even within the radiation region itself.

These observations clearly demonstrate the possibility of selective control over molecule clustering by IR lasers. At the same time, the method in question has a large number of unknown or poorly known parameters and characteristics, such as gas temperature and concentration in the jet, the rate of vibrational energy exchange between SF_6 isotopomers, and the evolution of these parameters along the jet propagation axis. To come to a higher selectivity of control over the clustering of SF_6 molecules among themselves and with argon atoms, all these factors need to be taken into consideration.

The studies carried out allowed the main parameters of isotope-selective suppression of the clustering of SF_6 molecules diluted in Ar to be obtained [41]. It was demonstrated that the use of a mixture of SF_6 molecular gas with argon as the carrier gas with the $SF_6/Ar \leqslant 1/200$ pressure ratio and the total gas pressure upstream of the nozzle in the range $p_\Sigma \approx 1.8-4$ atm permits us to observe selective suppression of the clustering of SF_6 molecules among themselves and with argon atoms.

The dependences of the degree and selectivity of SF_6 molecule clustering on the gas composition and pressure upstream of the nozzle and on the frequency and power of exciting laser radiation were obtained. It was shown that the degree of clustering suppression increases with radiation intensity, while selectivity decreases. Moreover, the resonant excitation of $^{32}SF_6$ molecules (at the 10P(16) laser line) suppresses the formation of $^{32}SF_6{}^{32}SF_6$ dimers, and the excitation of $^{34}SF_6$ molecules (at the 10P(34) line) suppresses the formation of $^{34}SF_6{}^{32}SF_6$ dimers.

The dependences of the degree of clustering suppression and selectivity on the distance between the particle radiation zone and the nozzle exit section were measured. It was shown that the highest efficiency and selectivity of the molecule clustering process is associated with particle excitation near the nozzle exit. As the laser beam moves away from the nozzle, the degree of clustering and selectivity sharply decreases, and IR cluster dissociation occurs upon transition into the advanced clustering region.

It was shown that control of the clustering of a mixture of SF_6 with Ar as the gas carrier allows relatively high enrichment and selectivity coefficients to be obtained. For example, a study of an SF_6/Ar mixture with a pressure ratio of 1/200 yielded a selectivity of $^{32}SF_6$ clustering relative to $^{34}SF_6$ of $\alpha(^{32}S/^{34}S) \geqslant 10-20$ in the jet irradiated at the laser 10P(16) line (frequency 947.74 cm^{-1}). The conditions are determined for the achievement of optimal efficacy and selectivity of suppression of molecule clustering .

The study demonstrated that control of the clustering of SF_6 molecules with Ar atoms ensures even better selectivity than control of the clustering of SF_6 molecules among themselves. For example, in the case of an $SF_6/Ar = 1/200$ mixture and jet irradiation at the 10P(16) laser line, selectivity of $^{32}SF_6$ clustering suppression relative to that of the $^{34}SF_6$ molecules amounts to $\alpha(^{32}S/^{34}S) \geqslant 25-30$. The selectivity values reported in [41] are 5–10 times those for SF_6 molecules in Refs [32–36]. The size of the spatial region in which selectivity of suppression of molecule clustering is realized has been determined. The length of this region under the conditions of the above experiments (nozzle output diameters of 0.25 and 0.16 mm) does not exceed 2–3 nozzle calibers.

6. Bromine-isotope-selective suppression of the clustering of CF_3Br molecules

6.1 Selective suppression of the clustering of CF_3Br molecules among themselves

6.1.1 Results of the first experiments. Reference [37] reports a study on the control of CF_3I molecule clustering that results from resonant vibrational excitation of molecules and clusters by IR radiation of a continuous CO_2 laser during the gas-dynamic expansion of a mixture of CF_3I molecular gas with argon and xenon as carriers. It was shown that the proposed method of control of the cluster-

ing process in molecular beams is applicable to isotope separation.

The first studies of the suppression of CF_3Br molecule clustering among the molecules themselves were performed in [38]. The molecule-cluster beam was detected by a time-of-flight mass spectrometer with laser UV ionization of particles. The pulsed nozzle had an exit orifice 0.22 mm in diameter. The half-height duration of the nozzle opening pulse was ≈ 400 μs, while gas pressure upstream of the nozzle varied within a range of 1.5–5 atm. The process of CF_3Br clustering was studied under experimental conditions and the gas parameters (pressure and composition) upstream of the nozzle exit at which intense molecule clustering occurs were determined. It was shown that molecular clusters failed to form in the beam if CF_3Br gas was used without a carrier at a pressure of less than 4 atm upstream of the nozzle. If the CF_3Br gas was mixed with Ar at a pressure ratio of $CF_3Br/Ar = 1/N$, where $N \geqslant 3$, and the total pressure upstream of the nozzle was higher than 1.5 atm, efficient $(CF_3Br)_m$ cluster formation in the jet was observed in the absence of free (unclustered) CF_3Br molecules.

Ionization of $(CF_3Br)_m$ clusters by UV laser radiation was induced at a wavelength having no exact resonance with free CF_3Br molecules ($\lambda_{UV} = 233.02$ nm), which allowed the clusters to be detected in the beam from ion signals of $^{79}Br^+$ and $^{81}Br^+$ atoms. At this wavelength, the free CF_3Br molecules practically avoided ionization. The selective action of CO_2 laser radiation on the cluster beam was also evaluated based on measurements of $^{79}Br^+$ and $^{81}Br^+$ ion signals.

It was shown [38] that, in the case of resonant vibrational excitation of gas-dynamically cooled CF_3Br molecules at the nozzle exit, it is possible to realize selective suppression of the clustering of CF_3Br molecules with respect to bromine isotopes. In experiments with the use of CF_3Br/Ar mixtures at the pressure ratios of 1/3 and 1/15, the factor of enrichment with bromine isotopes was $K_{enr}(^{79}Br) \approx 1.05 \pm 0.005$ and $K_{enr}(^{79}Br) \approx 1.06 \pm 0.007$, respectively, when the jet was irradiated at the 9R(30) laser line (1084.635 cm^{-1}).

6.1.2 Integrated research conditions. More detailed investigations of the suppression of the clustering of CF_3Br molecules among themselves under resonant excitation by radiation of a continuous-wave CO_2 laser were carried out in Ref. [39]. Molecules and clusters in the beam were detected by a quadrupole mass-spectrometer. The exit orifice of the pulsed nozzle was 0.22 mm in diameter, the half-height length of the nozzle opening pulse ranged between 400 and 600 μs, depending on gas pressure and composition, the gas pressure upstream of the nozzle varied from 1.5 to 3.0 atm, and the distance between the nozzle and the spectrometer was 250 mm.

Subsequent experiments [39] with gas mixtures at a $CF_3Br/Ar = 1/N$ pressure ratio, where $N = 10$, 30, 100, and 200, were carried out with regard to the data on $(CF_3Br)_m$ cluster formation and selectivity of suppression of CF_3Br clustering obtained in [38] and taking advantage of a quadrupole mass spectrometer for the detection and analysis of ion signals from Br_2^+ ($m/z = 158$, 160, 162 amu), $CF_3Br_2^+$ ($m/z = 227$, 229, 231 amu), and $(CF_3Br)_2^+$ ($m/z = 296$, 298, 300 amu) cluster fragments with and without jet irradiation by an IR laser. These measurements were used to calculate cluster beam enrichment (depletion) factor for bromine isotopes of interest and the degree of cluster depletion under the effect of jet irradiation.

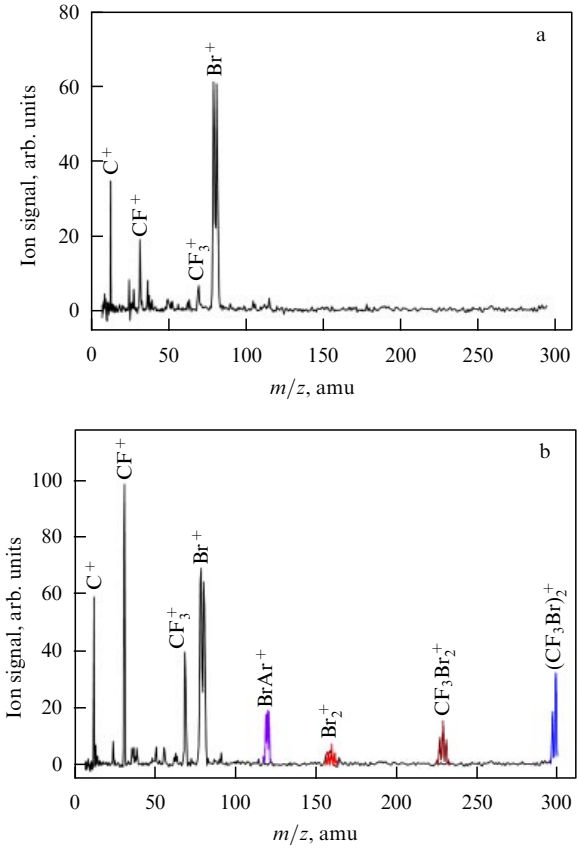

Figure 10. (a) Ion mass spectrum of CF_3Br molecules in a beam without a carrier gas. Gas pressure upstream of the nozzle is 4 atm. (b) Ion mass spectrum of CF_3Br/Ar mixture at pressure ratios of 1/30 and 1/100 ($m/z = 119-121$ amu). Total gas pressure upstream of the nozzle is 1.5 atm [39, 40].

Figures 10a, b present typical mass spectra of molecular (cluster) beams generated in experiments using CF_3Br gas without a carrier when the beam contains no clusters and with a carrier gas (argon) when the beam consists mostly of clusters. It can be seen that in the case of CF_3Br without a carrier at the pressure $p_0 \leqslant 4$ atm upstream of the nozzle, clusters fail to form in the beam (the mass spectrum lacks Br_2^+ ion peaks characteristic of $(CF_3Br)_m$ and other ion peaks of large cluster fragments. When CF_3Br is used with the carrier gas (Ar), the mass spectrum shows Br_2^+ ion peaks as well as ion peaks of $CF_3Br_2^+$ cluster fragments, and $(CF_3Br)_2^+$ dimers together with ion peaks of argon clusters, and mixed Ar_2^+, Ar_3^+, and $BrAr^+$ clusters. It is noteworthy that, if CF_3Br is used without a carrier gas, the ion signals of CF_3^+, CF^+, and C^+ fragments in the mass spectra are much weaker than Br^+ ion signals (Fig. 10a). At the same time, the use of CF_3Br with argon (when the probability of molecule clustering is especially high due to a stronger cooling of the gas), the ion peaks of CF_3^+, CF^+, and C^+ fragments are comparable with those of atomic bromine Br^+ (Fig. 10b), confirming that the expansion of CF_3Br in the presence of the Ar carrier gas is accompanied by molecule clustering [38]. The integral signals of the cluster ions measured with and without jet irradiation by a laser in [39] were used to calculate enrichment (depletion) factors for bromine isotopes in the beams and to determine the degree of cluster depletion.

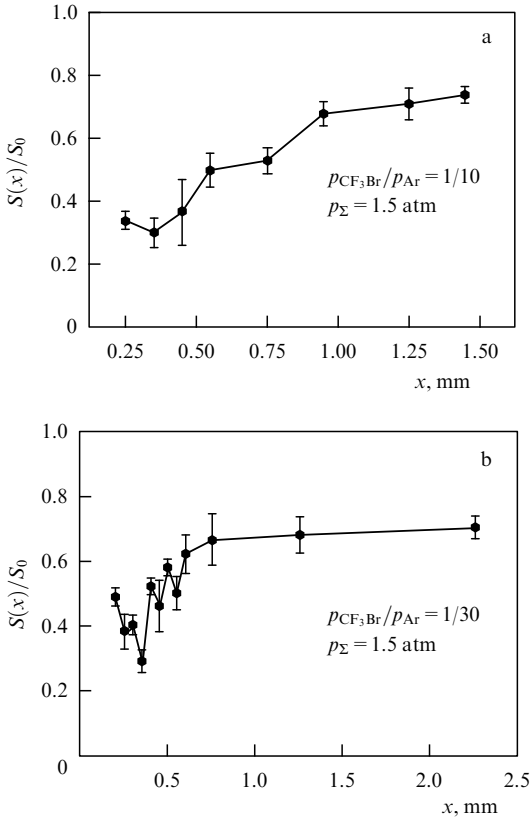

Figure 11. Normalized (a) Br_2^+ and (b) $(CF_3Br)_2^+$ ion signals versus distance between jet irradiation zone and nozzle exit for CF_3Br/Ar irradiation at pressure ratios (a) 1/10 and (b) 1/30. Total gas pressure upstream of the nozzle is 1.5 atm in both cases. CO_2 laser power (a) 5 W and (b) 5.1 W [39].

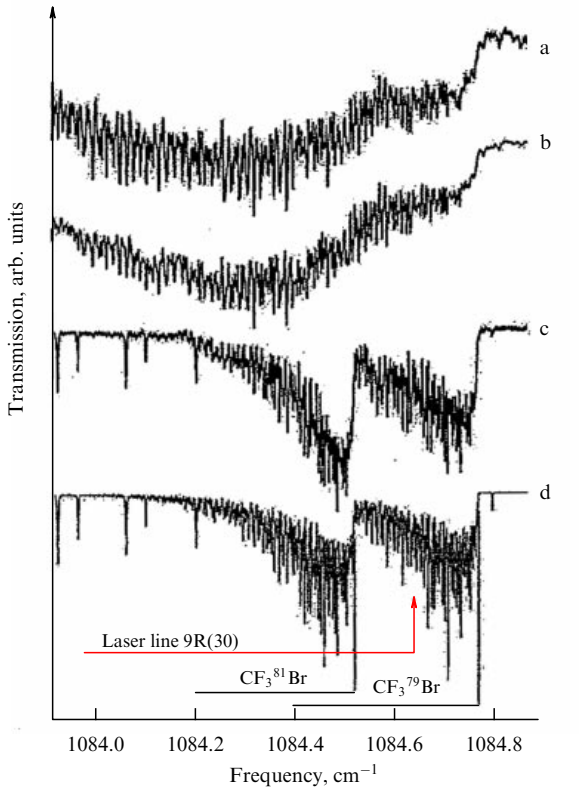

Figure 12. Spectra of the Q-branch of fundamental vibration ν_1 of CF_3Br molecules. Experimental spectrum of the gas in a cuvette (a) at room temperature, and (b) at 200 K; (c) experimental spectrum of the cooled gas in a free jet (averaged over 32 scanning procedures). (d) The calculated spectrum at $T = 50$ K (half-height width of 0.002 cm^{-1}) [65].

6.1.3 Results and their analysis. Figures 11a, b illustrate the action of IR radiation on a molecular cluster beam when using CF_3Br/Ar mixtures with a pressure ratio of 1/10 and 1/30, respectively. The total gas pressure upstream of the nozzle was 1.5 atm in both cases. Jet particles leaving the nozzle underwent irradiation by focused radiation of a continuous-wave CO_2 laser at a frequency of 1084.635 cm^{-1} (the 9R(30) line) and at different distances x from the nozzle exit section. This laser frequency is close to vibrational frequencies ν_1 of $CF_3{}^{79}Br$ and $CF_3{}^{81}Br$ molecules (1084.77 cm^{-1} and 1084.52 cm^{-1}), respectively [65]. It is located between the Q-branches of the IR absorption spectra of these molecules; at low gas temperatures in the jet, when the Q-branches are well resolved (Fig. 12), it occurs at the long wavelength end of the Q-branch of $CF_3{}^{79}Br$ molecules (detuning is roughly 0.134 cm^{-1}) [65]. Mass spectra of $^{79}Br_2^+$, $^{79}Br\,^{81}Br^+$, and $^{81}Br_2^+$ ion signals were obtained for each concrete position of point x at which jet particles were irradiated, as were those of other aforementioned ion cluster fragments with and without jet irradiation.

The $S(x)/S_0$ value in Figs 11a, b reflects a change in the number of ^{79}Br atoms in a cluster beam (normalized to the initial value S_0 of parameter $S(x)$ in a nonirradiated beam) as a result of jet irradiation by a laser, depending on the distance between the particle irradiation zone and the nozzle exit. $S(x)/S_0$ is actually the coefficient of cluster beam depletion in the ^{79}Br isotope. Notice that in the case of nonselective suppression of CF_3Br clustering, the same $S(x)/S_0$ value was observed in [39] for ^{81}Br atoms. Figure 11a presents the results of measurements of the Br_2^+ cluster ion signal ($m/z = 158$, 160, 162 amu) and Fig. 11b those of the $(CF_3Br)_2^+$ dimer ion signal ($m/z = 296$, 298, 300 amu). The $S(x)/S_0$ ratio was determined, taking into account the binomial distribution of bromine isotopes in the cluster fragments, from the relation

$$\frac{S(x)}{S_0} = \frac{(2I_{158} + I_{160})(\text{laser on})}{(2I_{158} + I_{160})(\text{laser off})}, \qquad (6.1)$$

where I_{158} and I_{160} are the intensities of $^{79}Br\,^{79}Br^+$ and $^{79}Br\,^{81}Br^+$ ion signals, respectively.

When a jet is irradiated at point $x = 0$, directly at the nozzle exit, with the laser beam coming in contact with the nozzle, the molecules are not yet cool enough, and their concentration remains high, which accounts for a large number of collisions. Therefore, notwithstanding that laser radiation excites here mostly $CF_3{}^{79}Br$ molecules, excitation affects $CF_3{}^{81}Br$ molecules too. As a result, all CF_3Br molecules, as well as atoms of the carrier gas, are strongly heated and cluster formation is markedly suppressed while the peaks of $^{79}Br_2^+$, $^{79}Br\,^{81}Br^+$, and $^{81}Br_2^+$ cluster fragments in the beam mass spectrum markedly diminish in height (Fig. 11a, b).

As the jet irradiation zone moves a distance of $0.25 \leqslant x \leqslant 0.75$ mm from the nozzle where molecules are cooled and clusters formed, selective suppression of the clustering becomes possible due to the low molecule concentration. There is practically no selectivity of IR emission at the

9R(30) line with respect to CF_3Br isotopomers usually contained in the newly formed clusters due to the superposition of IR absorption spectra of $CF_3{}^{79}Br$ and $CF_3{}^{81}Br$ isotopomers present in cluster 'packing' and the large width of the cluster IR absorption spectrum [81, 82]. This accounts for the suppression (including selective suppression) of molecule clustering and dissociation of small (nuclear) clusters in this region [1, 37, 38]. If the jet undergoes laser irradiation at distances $x \geqslant 1.0$ mm, nonselective dissociation of the formed clusters takes place [37, 38].

The small power of the laser accounts for a low probability of cluster dissociation (fragmentation). As a result, the amplitudes of $^{79}Br_2^+$, $^{79}Br\,^{81}Br^+$, and $^{81}Br_2^+$ ion peaks diminish but insignificantly in the case of jet irradiation (by roughly 25–30%) compared with their decrease in the absence of irradiation (Fig. 11a, b). To recall, the region in which maximum suppression of molecule clustering takes place narrows and shifts to the nozzle exit as the degree of CF_3Br dilution in argon increases. This process is related to accelerated cooling of CF_3Br molecules during gas-dynamic expansion as a result of higher dilution in the carrier gas. The region in which selective laser control of molecule clustering is possible also narrows and becomes displaced toward the nozzle exit section.

Therefore, the selective influence of IR radiation on the clustering of one of the chosen CF_3Br isotopomers can be observed only within a narrow range of distances between the nozzle and the irradiation zone where molecules are cooled and clusters begin to appear. In Figs 11a, b, this range is estimated as $x = 0.25-0.75$ mm. Just in this region the selective influence of IR radiation on cluster formation and, as a result, a more pronounced decrease in the $^{79}Br_2^+$ ion peak amplitude compared with that of $^{81}Br_2^+$ can be revealed.

Figure 13 shows mass spectra of $CF_3Br_2^+$ fragments ($m/z = 227$, 229, 231 amu) obtained without jet irradiation (Fig. 13a) and with irradiation by a CO_2 laser (5 W) at the 9R(30) line (frequency 1084.635 cm^{-1}) (Fig. 13b). The spectra are the result of averaging over ten spectrometric scanning procedures in the said range of mass numbers with a 0.05-amu resolution. The jet was irradiated at distance $x = 0.35$ mm from the nozzle. Laser radiation at this line is strongly absorbed by $CF_3{}^{79}Br$ molecules. Evidently, jet irradiation causes a much more pronounced decrease in the $CF_3{}^{79}Br_2^+$ cluster ion signal ($m/z = 227$ amu) than that of $CF_3{}^{81}Br_2^+$ ($m/z = 231$ amu). This finding confirms suppression of $CF_3{}^{79}Br$ clustering for laser-induced resonant excitation of the molecules at the nozzle exit. This process is associated, in accordance with the binomial distribution in peak intensities, with a more pronounced decrease in the $CF_3{}^{79,81}Br_2^+$ ion signal ($m/z = 229$ amu) compared with the $CF_3{}^{81}Br_2^+$ ion signal.

Figure 14 presents the results of determination of the enrichment factor $K_{enr}(^{79}Br)$ for a CF_3Br/Ar mixture at the pressure ratios of (a) 1/10 and (b) 1/30 and the total gas pressure upstream of the nozzle of 1.5 atm. The data shown in Figs 14a, b were obtained by detecting cluster ion signals from molecular bromine Br_2^+ ($m/z = 158$, 160, 162 amu) and $(CF_3Br)_2^+$ dimer signals ($m/z = 296$, 298, 300 amu), respectively. The jet was irradiated at the 9R(30) laser line (frequency 1084.635 cm^{-1}). The factor of cluster beam enrichment $K_{enr}(^{79}Br)$ with ^{79}Br isotopes was determined as the ratio of concentrations of bromine isotopes in the CF_3Br/Ar mixture measured in the beam mass spectra after irradiation of the molecular jet by a CO_2 laser divided by the same ratio measured before irradiation. Concentrations of bromine atoms before and after jet irradiation were regarded as proportional to the respective ion signals in the mass spectrum. Hence,

$$K_{enr}(^{79}Br) = \frac{\left[(2I_{158} + I_{160})/(2I_{162} + I_{160})\right](\text{laser on})}{\left[(2I_{158} + I_{160})/(2I_{162} + I_{160})\right](\text{laser off})}, \quad (6.2)$$

where I_{158}, I_{160}, and I_{162} are the intensities of ion signals from $CF_3{}^{79}Br_2^+$, $CF_3{}^{79}Br\,^{81}Br^+$, and $CF_3{}^{81}Br_2^+$, respectively.

To determine ion signals in (6.2) and other ion signals, the ion peaks obtained in our experiments were approximated by Gaussian curves (Figs 13a, b) and areas under the peaks were determined by integration. Selectivity of suppression of CF_3Br clustering was assessed as the ratio of the probability of suppressing $CF_3{}^{79}Br$ clustering to that of $CF_3{}^{81}Br$ clustering, i.e., $\alpha = \beta_{79}/\beta_{81}$. The values of β_{79} and β_{81} reflect, by analogy with the molecule dissociation yield [14, 17], the relative depletion of the cluster beam being detected in $CF_3{}^{79}Br$ and $CF_3{}^{81}Br$ molecules.

Because laser irradiation of the jet selectively suppresses $CF_3{}^{79}Br$ clustering, the enrichment coefficient derived from relation (6.2) is less than unity. In our case, the cluster beam is depleted of ^{79}Br atoms and enriched with ^{81}Br. The coefficient of enrichment of the cluster beam with ^{81}Br is the inverse of $K_{enr}(^{79}Br)$. Figure 14a shows that the estimated value of the

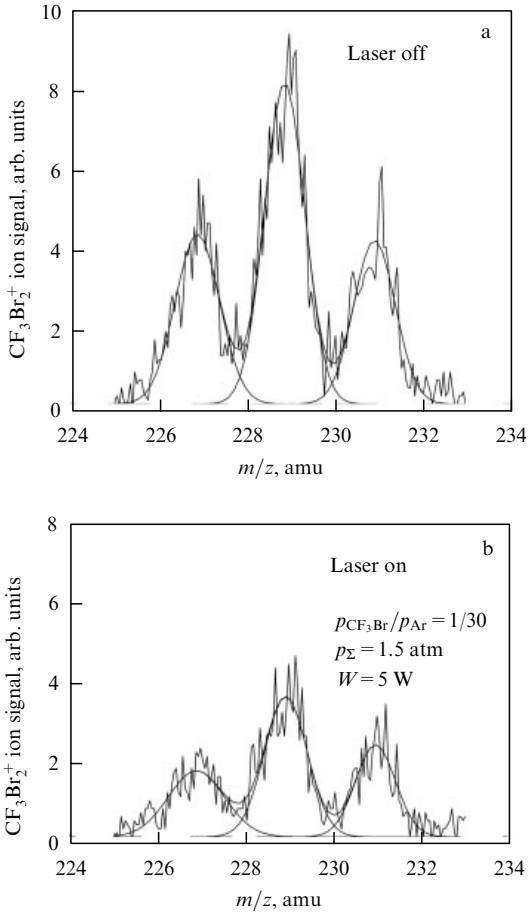

Figure 13. $CF_3Br_2^+$ ion signals ($m/z = 227$, 229, and 231 amu (a) without and (b) with jet irradiation by a laser at 5 W. A CF_3Br/Ar mixture was used at the pressure ratio of 1/30 and total pressure upstream of the nozzle 1.5 atm. The jet was irradiated at the distance $x = 0.35$ mm from the nozzle. Approximation of experimental data by Gaussian curves is shown.

Table 2. Results of selective suppression of the clustering of CF_3Br molecules among themselves (from Ref. [39]) and with argon atoms (from Ref. [40], highlighted in bold) during the gas-dynamic expansion of a CF_3Br/Ar mixture under different experimental conditions. The jet was irradiated by a CO_2 laser at the 9R(30) line (frequency 1084.365 cm^{-1}). Total gas pressure upstream of the nozzle: 1.5 atm.

$\frac{p_{CF_3Br}}{p_{Ar}}$	Laser power, W	Ion peak measured	Mass number m/z, amu	Residual signal	Enrichment factor $K_{enr}(^{79}Br)$	Selectivity $\alpha(^{81}Br/^{79}Br)$	Nozzle pulse length, μs	Distance x from the irradiation zone to the nozzle, mm
1/10	5.0	Br_2^+	(158), (160), (162)	0.37 ± 0.11	0.84 ± 0.07	1.18 ± 0.04	450	0.45
1/10	4.9	$CF_3Br_2^+$	(227), (229), (231)	0.38 ± 0.03	0.98 ± 0.03	1.03 ± 0.02	450	0.55
1/30	5.0	$CF_3Br_2^+$	(227), (229), (231)	0.47 ± 0.02	0.95 ± 0.02	1.12 ± 0.01	450	0.45
1/30	5.1	$(CF_3Br)_2^+$	(296), (298)	0.31 ± 0.04	0.90 ± 0.06		450	0.45
1/100	**4.6**	$\mathbf{BrAr^+}$	**(119), (121)**	$\mathbf{0.62 \pm 0.07}$	$\mathbf{0.67 \pm 0.05}$	$\mathbf{4.02 \pm 0.19}$	**600**	**0.45**
1/100	3.9	$(CF_3Br)_2^+$	(296), (298)	0.54 ± 0.08	0.90 ± 0.05		450	0.45
1/200	**3.8**	$\mathbf{BrAr^+}$	**(119), (121)**	$\mathbf{0.67 \pm 0.09}$	$\mathbf{0.77 \pm 0.09}$	$\mathbf{2.31 \pm 0.11}$	**600**	**0.3**
1/200	3.8	$(CF_3Br)_2^+$	(296), (298)	0.59 ± 0.03	0.88 ± 0.04		600	0.3

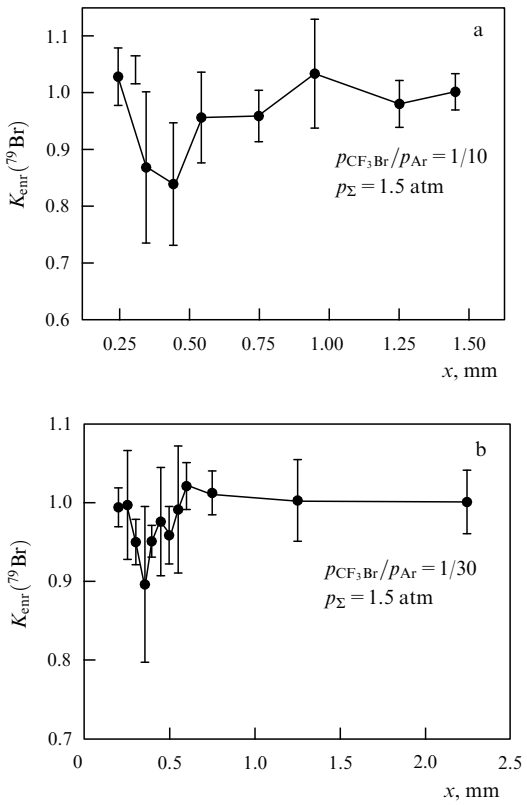

Figure 14. Dependences of enrichment factor $K_{enr}(^{79}Br)$ on the distance between particle irradiation zone and nozzle exit for a CF_3Br/Ar mixture with pressure ratios of (a) 1/10 and (b) 1/30. CO_2 laser power is (a) 5 W and (b) 5.1 W. Total gas pressure is 1.5 atm in both cases [39].

enrichment coefficient $K_{enr}(^{79}Br) \approx 0.84 \pm 0.07$ is achieved at point $x = 0.45$ mm when selectivity is $\alpha \approx 1.18$. Similarly, for the $CF_3Br/Ar = 1/30$ mixture, the estimated value of the enrichment factor $K_{enr}(^{79}Br) \approx 0.89 \pm 0.06$ ($\alpha \approx 1.12$). It is achieved at point $x = 0.35$ mm, while at the point $x = 0.5$ mm the selective influence of IR radiation on molecule clustering almost does not manifest itself. For the $CF_3Br/Ar = 1/10$ mixture, the region of clustering control by IR radiation is larger ($\Delta x \approx 0.55$ mm).

Results of the measurement of beam enrichment factors and degrees of depletion are presented in Table 2. For comparison, it includes some data from Ref. [40] on control of CF_3Br clustering with argon atoms (see Section 6.2). The highest enrichment factors $K_{enr}(^{81}Br)$ of cluster beam with ^{81}Br atoms were recorded for mixtures of $CF_3Br/Ar = 1/10$ and $CF_3Br/Ar = 1/30$ when Br_2^+ and $(CF_3Br)_2^+$ cluster ion fragments were detected. These signals decreased by approximately 60% and 45%, respectively, in comparison with the signals in the nonirradiated beam.

The enhanced dilution of the molecular gas in the carrier gas could be expected to increase enrichment factors due to the strong cooling of the gas and the narrowing of the molecule absorption spectra, as well as due to the decreased rate of vibrational energy exchange between $CF_3{}^{79}Br$ and $CF_3{}^{81}Br$ isotopomers. However, the authors of Ref. [39] failed to confirm this observation, probably because an increased degree of gas dilution leads to a significant reduction (collapse) in the range within which molecule clustering control is still possible. As a result, the area where the effect is localized becomes much smaller than the laser spot (≈ 0.5 mm) (Figs 11a, b). It eventually worsens the selectivity of clustering control.

6.2 Selective suppression of the clustering of CF_3Br molecules with argon atoms

6.2.1 Experimental conditions. The formation of mixed $(CF_3Br)_mAr_n$ clusters, unlike the generation of homogeneous ones, $(CF_3Br)_m$, requires a much greater cooling of particles in the expanding jet, because the energy of binding of CF_3Br molecules among themselves in a homogeneous $(CF_3Br)_m$ cluster ($\approx 0.25-0.3$ eV [71]) is significantly higher than the energy of binding between CF_3Br molecules and argon atoms in a mixed $(CF_3Br)_mAr_n$ cluster ($\leqslant 0.1$ eV [1, 44]). This means that the jet temperature for the formation of mixed $(CF_3Br)_mAr_n$ clusters must be much lower than for the generation of homogeneous $(CF_3Br)_m$ clusters [83]. With this in mind, the authors of Ref. [40] used highly diluted mixtures of the molecular gas CF_3Br in argon for the assessment of selective suppression of CF_3Br clustering with Ar atoms. CF_3Br/Ar mixtures at pressure ratios of 1/100 and 1/200 were used for the purpose, the total gas pressure upstream of the nozzle being 1.5 atm.

With such parameters of the gas upstream of the nozzle, a rather efficient formation of mixed clusters containing a small number ($m = 1-2$) of CF_3Br molecules took place, whereas the probability of formation of large homogeneous $(CF_3Br)_m$ clusters was insignificant [78]. Moreover, the small total gas pressure upstream of the nozzle and strong dilution of the molecular mixture in the carrier gas facilitated the achievement of higher values of separation parameters (selectivity and enrichment coefficients) for the molecule clustering process. Under conditions of high total gas pressure upstream of the nozzle and low dilution, the processes of gas heating and vibrational energy exchange between CF_3Br isotopomers lead to a decrease in selectivity and enrichment factors [38, 39].

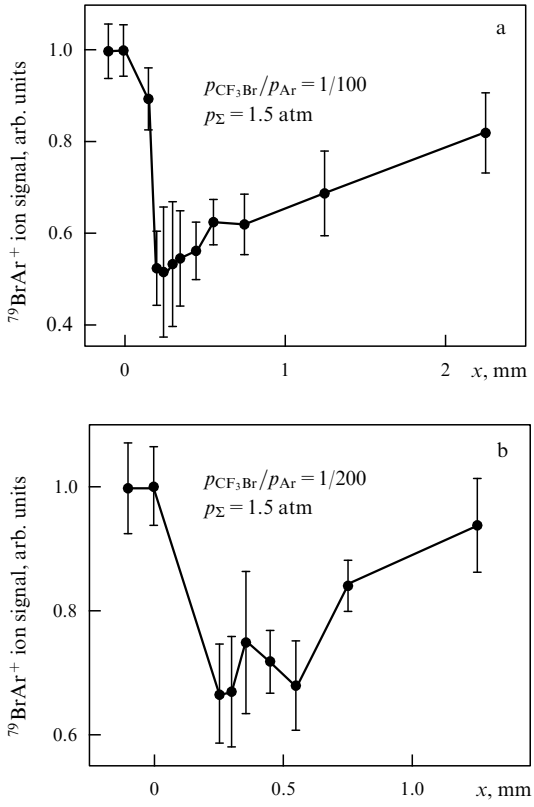

Figure 15. Dependences of the $^{79}BrAr^+$ ion signal normalized to the signal strength in a nonirradiated jet on distance x between particle irradiation zone and nozzle exit for a CF_3Br/Ar mixture at pressure ratios of (a) 1/100 and (b) 1/200. Total gas pressure is 1.5 atm in both cases [40].

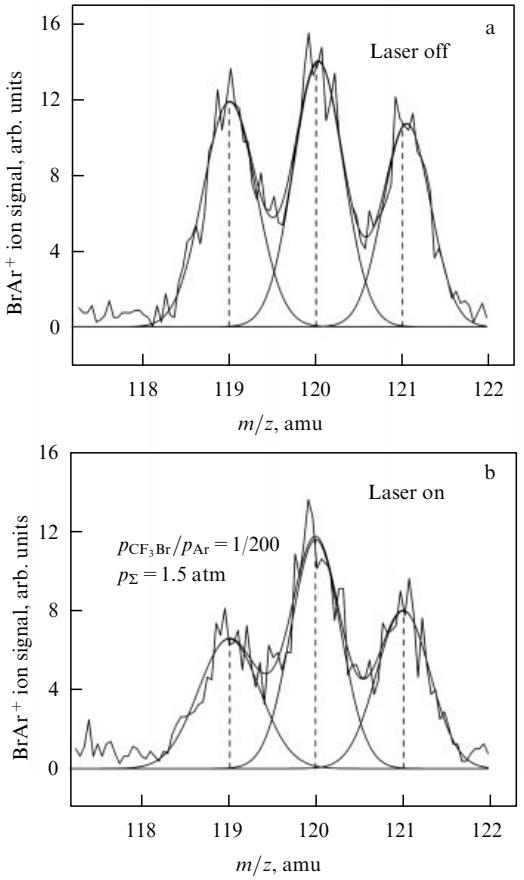

Figure 16. Mass spectra of $^{79}BrAr^+$, Ar_3^+, and $^{81}BrAr^+$ cluster fragments ($m/z = 119$, 120, and 121 amu) (a) without and (b) with irradiation by a CO_2 laser at line 9R(30) (frequency 1084.635 cm^{-1}) and radiation power ≈ 3.8 W. The CF_3Br/Ar mixture with a pressure ratio of 1/200 and total pressure of 1.5 atm upstream of the nozzle was used. The jet was irradiated at the distance $x = 0.3$ mm from the nozzle. Experimental spectra are approximated by Gaussian curves [40].

6.2.2 Results of the studies and their analysis. The experiments described in [40] were designed to measure and analyze ion signals from mixed $BrAr^+$ cluster fragments ($m/z = 119$ and 121 amu) without jet irradiation and after irradiation by a CO_2 laser. The data thus obtained were used to calculate factors of cluster beam enrichment with and depletion of the selected bromine isotopes under the effect of laser irradiation of the jet. The ion peak of Ar_3^+ ($m/z = 120$ amu) clusters was invariably detected in the mass spectrum between the $^{79}BrAr^+$ ($m/z = 119$ amu) and $^{81}BrAr^+$ ($m/z = 121$ amu) cluster fragments (see Figs 16a, b below).

Figure 15 illustrates the influence of IR radiation on the molecular cluster beam when the CF_3Br/Ar mixture was used at the (a) 1/100 and (b) 1/200 pressure ratios. It shows dependences of the $^{79}BrAr^+$ cluster ion signal normalized to its strength in the nonirradiated jet at distance x of the jet irradiation zone from the nozzle. The total gas pressure upstream of the nozzle was 1.5 atm in both cases. The particles escaping from the nozzle were irradiated by the focused CO_2 laser emission at a frequency of 1084.635 cm^{-1} (laser line 9R(30)) at different distances x from the nozzle. The mass spectra of $^{79}BrAr^+$, Ar_3^+, and $^{81}BrAr^+$ ($m/z = 119$, 120, and 121 amu) ion signals were found for each concrete position of the irradiation zone (x value).

When the jet was irradiated at point $x = 0$ directly on the nozzle, where the laser beam touched its exit section, the molecules were not yet sufficiently cool, while their concentration and collision rate were quite high. CO_2 laser radiation heated all CF_3Br molecules as well as atoms of the carrier gas. Simultaneously, the cluster formation process was significantly suppressed and ion peaks of $^{79}BrAr^+$ and $^{81}BrAr^+$ cluster fragments in the beam mass spectrum markedly decreased (see Fig. 15).

Figure 16 shows mass spectra of $^{79}BrAr^+$, Ar_3^+, and $^{81}BrAr^+$ ($m/z = 119$, 120, and 121 amu) cluster fragments obtained in the absence of jet irradiation (Fig. 16a) and with irradiation by a CO_2 laser on line 9R(30) (frequency 1084.635 cm^{-1}) at a radiation power of ~ 3.8 W (Fig. 16b). A CF_3Br/Ar mixture was used with a pressure ratio of 1/200. The total gas pressure upstream of the nozzle was 1.5 atm. The jet was irradiated at distance $x = 0.3$ mm from the nozzle. Laser radiation at line 9R(30) was most extensively absorbed by $CF_3{}^{79}Br$ molecules. Figure 16 shows that jet irradiation caused a much more pronounced decrease in the $^{79}BrAr^+$ ($m/z = 119$ amu) cluster ion signal than that of the $^{81}BrAr^+$ ($m/z = 121$ amu) signal. Similar results were obtained in [40] for the CF_3Br/Ar mixture at the 1/100 pressure ratio and a total pressure of 1.5 atm upstream of the nozzle. These data confirm selective suppression of $CF_3{}^{79}Br$ clustering with argon atoms.

Figure 17 presents the results of determining enrichment factors $K_{enr}(^{79}Br)$ in a cluster beam in a study with the use of a CF_3Br/Ar mixture at the pressure ratios of (a) 1/100 and (b) 1/200 and a total gas pressure upstream of the nozzle of 1.5 atm in both cases. The results were obtained for the case of

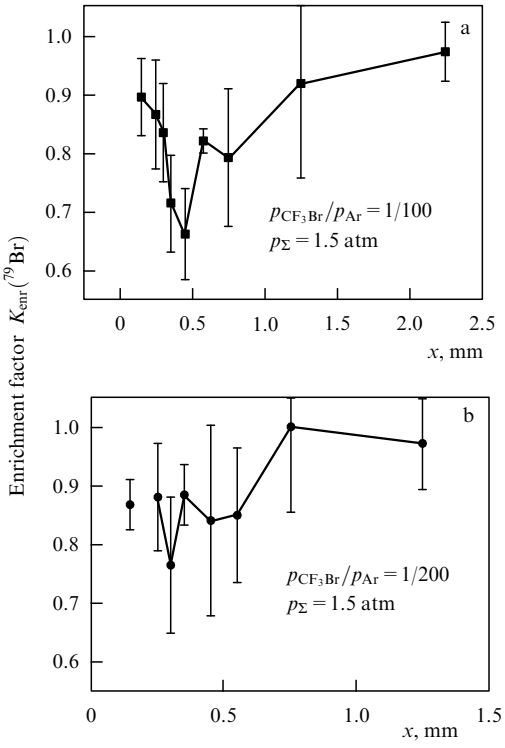

Figure 17. Dependences of enrichment factor $K_{enr}(^{79}Br)$ on distance between jet irradiation zone and nozzle exit for a CF_3Br/Ar mixture with pressure ratios of (a) 1/100 and (b) 1/200 at a CO_2 laser power of (a) 4.6 W and (b) 3.8 W. Total gas pressure upstream of the nozzle is 1.5 atm in both cases [40].

detection of $^{79}BrAr^+$ and $^{81}BrAr^+$ ($m/z = 119$ and 121 amu) mixed cluster ion signals and averaging of the data from a series of ten measurements of mass-spectra intensities. The jet was irradiated at the 9R(30) laser line (frequency 1084.635 cm^{-1}). The factor of enrichment $K_{enr}(^{79}Br)$ of the cluster beam with ^{79}Br isotope was determined as the ratio of bromine isotope concentrations contained in mixed $(CF_3Br)_mAr_n$ clusters and measured after molecular jet irradiation by the CO_2 laser divided by the ratio of initial bromine concentrations in the CF_3Br/Ar mixture measured in the beam mass spectra prior to irradiation. Concentrations of bromine atoms before and after jet irradiation were assumed to be proportional to the respective ion signals in the beam mass spectrum prior to irradiation. It can be concluded that

$$K_{enr}(^{79}Br) = \frac{(I_{119}/I_{121})(\text{laser on})}{(I_{119}/I_{121})(\text{laser off})}, \qquad (6.3)$$

where I_{119} and I_{121} are the intensities of $^{79}BrAr^+$ and $^{81}BrAr^+$ ion signals, respectively. To determine ion signals in (6.3), the experimental ion peaks obtained in our studies were approximated by Gaussian curves (Figs 16a, b), and the areas under them were determined by integration. Selectivity α of suppression of CF_3Br clustering with argon atoms was evaluated as the ratio of the probability of suppression of $CF_3{}^{79}Br$ clustering to that of $CF_3{}^{81}Br$ clustering, i.e., $\alpha = \beta_{79}/\beta_{81}$. β_{79} and β_{81} values reflect the relative loss of $CF_3{}^{79}Br$ and $CF_3{}^{81}Br$ molecules from the mixed $(CF_3Br)_mAr_n$ clusters of the beam being detected.

Table 2 presents the results of assessment of enrichment factors, selectivities, and degrees of beam depletion in ^{79}Br isotopes (residual ion signals of $^{79}BrAr^+$) obtained by measuring the aforementioned cluster ion peaks under the concrete experimental conditions. The data are presented together with the results of Ref. [39] on controlling the clustering of CF_3Br molecules among themselves. It follows from these data that control over CF_3Br clustering with argon atoms allows obtaining much higher factors of enrichment and selectivity than the control of the clustering of CF_3Br molecules among themselves, one of the possible causes being a much higher temperature at which clustering of the molecules among themselves in a jet occurs than the temperature of the clustering between the molecules and argon atoms. It accounts for the higher optical selectivity of CF_3Br excitation (hence, selectivity of molecule clustering suppression) in the latter case than that in the former one.

6.3 Selected estimates and relevant remarks

Let us make some estimates (by analogy with estimates in Section 5.4) to understand the relationship between parameters of the process under study. It was shown based on the IR absorption spectrum of laser-excited CF_3Br isotopomers at low (~ 50 K) temperature (see Fig. 12) and the small width of the laser radiation spectrum ($\leqslant 100-150$ MHz) that the optical selectivity of $CF_3{}^{79}Br$ excitation with respect to $CF_3{}^{81}Br$ at the line 9R(30) frequency is $\alpha_{exc}(^{79}Br/^{81}Br) \approx 25-30$. Selectivities observed in [38–40] are significantly worse than that. The causes of selectivity deterioration, as in the case of selective suppression of SF_6 clustering, are the vibrational energy exchange between $CF_3{}^{79}Br$ and $CF_3{}^{81}Br$ during particle excitation near the nozzle where molecule concentration is especially high, the elevated (over 50 K) temperature of particles in the irradiation zone responsible for the significantly lower optical selectivity of particle excitation compared with the above value, and the relatively large size of the laser spot (roughly 0.5 mm in diameter) resulting in a much larger particle irradiation zone than the region of maximum selectivity of molecule excitation. There is little doubt that all these factors affect the selectivity of the process in question.

The main objective of studies [38–40] was to evaluate bromine isotope-selective suppression of CF_3Br molecule clustering among themselves and with argon atoms by CO_2 laser radiation. In our opinion, the data obtained convincingly demonstrate such a possibility. At the same time, many unknown and/or poorly understood characteristics and parameters of the method remain to be elucidated. They include gas temperature and concentration in the jet, the structure of IR absorption spectra of CF_3Br isotopomers near the frequency at which they are excited by a laser, and the rate of vibrational energy exchange among CF_3Br isotopomers. To obtain higher values of isotope separation parameters (efficiency and selectivity) by the method in question, all these factors need to be taken into consideration.

Isotope-selective suppression of the clustering of molecules among themselves and with argon atoms can be used in principle to design the isotope separation process. One of the conceivable variants of its implementation includes two stages. The first is selective suppression of the clustering of the chosen isotopic modification of the molecules leading to their distribution in the beam at a larger solid angle than that of the distribution of colder and heavier clusters containing nontarget molecules. The second is the spatial separation of target molecules from the cluster beam. Such a scheme to achieve the maximum separation coefficient requires not only

high optical selectivity of IR excitation of the necessary isotopic modifications of the molecules but also a high enough selectivity during the spatial separation of target molecules from the cluster beam.

7. Isotope-selective IR dissociation of $(SF_6)_m Ar_n$ van der Waals clusters

7.1 Certain remarks and details of the experiment

Isotope-selective IR dissociation of van der Waals molecules as exemplified by $(SF_6)_m Ar_n$ complexes (where $1 \leqslant m \leqslant 3$, $1 \leqslant n \leqslant 9$) was investigated in some detail in earlier studies [33–36]. These complexes formed in a free jet during expansion of the mixture of SF_6 molecules with argon through a nozzle 0.1 mm in diameter at an SF_6 partial pressure of 0.5%. Isotope-selective dissociation of the clusters was demonstrated. For example, irradiation of a natural mixture of SF_6 isotopomers diluted in Ar by a continuous-wave CO_2 laser yielded factors of enrichment K_{enr} and selectivity α with respect to $^iSF_6$ ($i = 32$, 34) equaling $K_{enr} \approx 1.3$ and $\alpha(32/34) \approx 1.2$, respectively [33, 36]. The dependences of enrichment factors on the frequency of exciting laser radiation were deduced. It was shown that a proper choice of the radiation wavelength allows obtaining beams either enriched with or depleted of the selected isotopomers.

The possibility of using the method of IR vibrational predissociation of van der Waals clusters to separate uranium isotopes was considered in Ref. [7]. The main objective of recent study [42] was to evaluate the possibility of improving characteristics of the separation (efficiency and selectivity) compared with those presented in earlier studies [33, 35, 36]. Reference [42] reports a detailed study of isotope-selective dissociation of small homogeneous and mixed $(SF_6)_m Ar_n$ clusters in the beam, measuring the dependences of the efficacy and selectivity of their dissociation on gas parameters upstream of the nozzle and characteristics of laser radiation and finding out the optimal conditions for the achievement of maximum efficiency and selectivity of cluster dissociation.

The authors of [42] made use of pulsed nozzles with an orifice diameter of 0.16 or 0.25 mm. The half-height length of the nozzle opening pulse varied from 0.3 to 1.6 ms, depending on the gas pressure and composition upstream of the nozzle. Gas pressure upstream of the nozzle ranged from 1.3 to 3.0 atm. The distance between the nozzle exit section and the QMS ionization chamber was 570 mm.

7.2 Choice of conditions for measurements and technical results

It was mentioned in Section 4.2 that small-size clusters (including mixed ones) need to be used for maximum selectivity of their dissociation. This requires a strong dilution of studied molecules in the carrier gas and the adequate choice of optimal gas pressure upstream of the nozzle and the site of gas flow irradiation. The last requirement implies flow irradiation at earlier stages of cluster formation. A strong dilution of molecules by atomic gasses leads to the formation of mixed clusters which, in turn, causes an additional broadening of the IR absorption spectra and cluster dissociation [33, 63]. To choose the optimal conditions for measurements, the authors of Ref. [42] analyzed IR absorption spectra of homogeneous and mixed $(SF_6)_m Ar_n$ clusters [34, 62–64] and carried out a number of preliminary experiments.

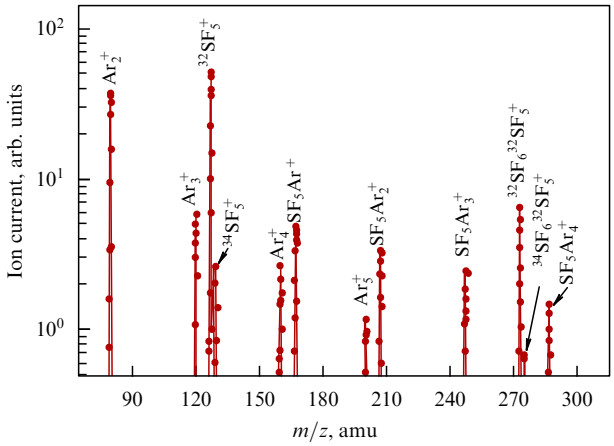

Figure 18. Part of the mass spectrum of cluster beam ionization products in a range of masses $70 \leqslant m/z \leqslant 300$ amu. An SF_6/Ar mixture at a pressure ratio of 1/200 and total gas pressure 2.4 atm was used [42].

A characteristic mass spectrum obtained with the use of an SF_6/Ar mixture at a pressure ratio of 1/200 is presented in Fig. 18. It was shown in [78] that in this case Ar clusters and mixed $(SF_6)_m Ar_n$ clusters with the number of particles $m \leqslant 3$ and $n \leqslant 9$ are generated in the beam. Fragment Ar_k^+ ions ($k = 2-5$) and fragment ions of other products are well apparent in Fig. 18, suggesting the generation of mixed clusters like $(SF_6)_m Ar_n$. Specifically, these are fragment $SF_5Ar_l^+$ ions ($l = 1-4$) and some others. The most pronounced is the SF_5^+ ion peak to which both cluster ionization fragments and free (unclusterd) SF_6 monomer ionization contribute. A quite essential finding is a peak with the mass number $m/z = 273$, corresponding to the $^{32}SF_6{}^{32}SF_5^+$ ion fragment resulting from $(^{32}SF_6)_2$ dimer dissociation. A contribution to this peak may just as well come from the fragments of larger clusters like $(SF_6)_2 Ar_n$. However, they could not be registered directly in Ref. [42] due to the limited range of mass recording by the QMS ($m/z \leqslant 300$).

Variations in the cluster constituent intensity in the beam associated with jet excitation by the IR laser in the region of cluster formation and/or existence were measured by a QMS from the behavior of (reduction in) the signals from $SF_6SF_5^+$, SF_5Ar^+, and SF_5^+ ion products and their isotope components. The QMS could be operated in two regimes: one for measuring the panoramic spectrum of the ion fragments being formed at a given point in time, the other (the time-of-flight regime, with the QMS tuned to a certain mass) for the measurement of evolution of the ion signal in time with the arrival of particles in the QMS ionization chamber.

Most experiments were made using argon as the carrier gas. Preliminary experiments with an SF_6/Ar mixture allowed choosing the working range of mixture pressure upstream of the nozzle and the degree of gas dilution ($p_\Sigma = 1.3-2.2$ atm and $SF_6/Ar = 1/80-1/200$, respectively). The nozzle orifice diameter was 0.16 mm.

As was shown in Section 5.1 (see Fig. 3), the excitation of an SF_6 molecular cluster jet near the nozzle causes an appreciable weakening of the cluster signal. As the distance between the nozzle and the excitation zone increases, the signal recovers partly (up to 80% of the initial value) and thereafter remains unaltered. The observed dip corresponds

to the SF_6 clustering suppression region as a result of vibrational excitation of the molecules [37, 38, 77]. An increase in the distance between the nozzle and the particle irradiation zone is associated with the transition to the region of advanced and 'frozen' condensation; therefore, the decrease in the ion signal in this region is attributable, first and foremost, to cluster dissociation [37, 38, 77].

To realize selective dissociation of $(^{32}SF_6)_2$ dimers, the authors of [42] chose the 10P(34) laser line (frequency 931.00 cm^{-1}). This frequency is detuned from the center of the absorption band of free $^{32}SF_6$ molecules [60] but coincides with the low-frequency absorption band of $(^{32}SF_6)_2$ dimers [62–64]. The SF_6/Ar mixture was used at a pressure ratio of 1/200 and the total gas pressure upstream of the nozzle equaled 1.5 atm to ensure the presence of a large dimer fraction in the beam.

At the beginning, the jet was irradiated near the nozzle exit where the number of dimers had to be minimal. Results of the measurement are presented in Fig. 19a. It shows some decrease in all ion peaks, despite the lack of resonance with free (unclustered) $^{32}SF_6$ molecules, which were expected to predominate in this jet region. The red curve *2* corresponding (in the case of an irradiated jet) to the fractional contributions from the respective sulfur isotopes $q = (0.86, 0.86, 0.86)$ is in excellent agreement with experiment, which suggests the absence of selectivity. As to ion peak reduction note that the laser beam diameter was ≈ 0.5 mm, or roughly three nozzle calibers. Therefore, part of the laser beam occurred in the spatial region where molecule clustering began and thereby caused the cluster signal to decrease as a result of suppression of the molecule clustering process [37, 38, 77].

When the jet is irradiated 2 mm from the nozzle exit, i.e., in the region where molecule clustering is virtually completed (see Fig. 3), the natural isotope ratio is markedly changed (Fig. 19b). In the case of dimer dissociation, the selectivity parameter α can be introduced as the ratio of probabilities of $^{32}SF_6{}^{32}SF_6$ and $^{34}SF_6{}^{32}SF_6$ cluster dissociation. Then, the data in Fig. 19b give the estimated value of selectivity $\alpha \approx 2$.

The selectivity of $^{32}SF_6{}^{32}SF_6$ cluster dissociation relative to that of $^{34}SF_6{}^{32}SF_6$ clusters even more clearly manifests itself when the particles are irradiated in the 'frozen' beam region and the clustering process is practically completed. This inference ensues from Fig. 19c, showing mass spectra of the $SF_6SF_5^+$ dimer ion fragment with its isotopic modifications without jet irradiation and with its irradiation at the 10P(34) laser line (frequency 931.00 cm^{-1}) 7 mm from the nozzle (cf. Fig. 3).

It follows from Fig. 19c that the $^{32}SF_6{}^{32}SF_5^+$ ion signal significantly (by more than 20%) decreases, whereas the $^{34}SF_6{}^{32}SF_5^+$ signal remains unaltered (within the statistical error), which formally corresponds to 'infinite' selectivity. Taking account of the measurement error, the estimate value of $(^{32}SF_6)_2$ dimer dissociation selectivity with respect to $^{34}SF_6{}^{32}SF_6$ dimers is $\alpha \geqslant 20-25$ [42].

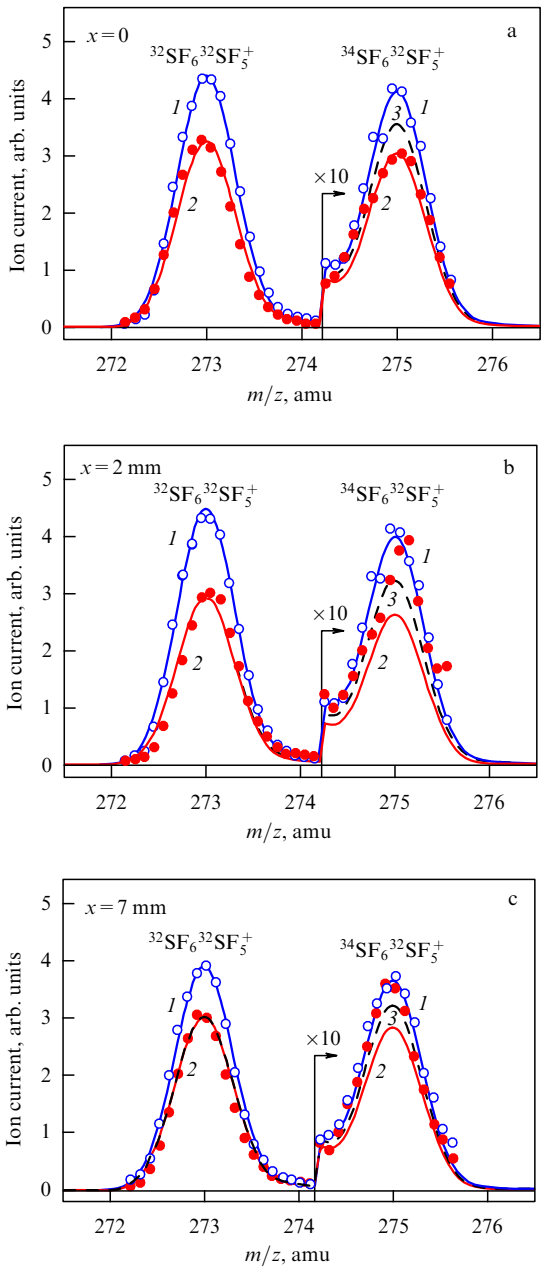

Figure 19. (Color online.) (a) Mass spectra in the region of an $SF_6SF_5^+$ dimer ion fragment with its isotopic modifications. Solid circles are irradiation. Blue curves *1*: $q = (1, 1, 1)$. Red curves *2*: (a) $q = (0.86, 0.86, 0.86)$; (b) $q = (0.83, 0.83, 0.83)$; (c) $q = (0.88, 0.88, 0.88)$. Dashed curves *3*: (a) $q = (0.86, 1, 1)$; (b) $q = (0.83, 1, 1)$; (c) $q = (0.88, 1, 1)$ (in the 273 amu region, curves *3* coincide with the red curves *2*). SF_6/Ar gas mixture was used upstream of the nozzle with a pressure ratio of 1/200 and total gas pressure 1.63 atm. Nozzle diameter was 0.16 mm. Laser power was 4.6 W. Distances from the nozzle: (a) 0 (part of the laser beam comes into contact with the nozzle), (b) 2 mm, and (c) 7 mm [42].

7.3 Dependence of IR cluster dissociation parameters on the distance of the particle irradiation zone from the nozzle exit section. The influence of gas dilution

The main approach to determining the efficiency and selectivity of cluster dissociation by IR laser radiation [42] consists of the measurement of intensity of $^{32}SF_6{}^{32}SF_5^+$ and $^{34}SF_6{}^{32}SF_5^+$ ion product signals, depending on the distance between the nozzle exit and the particle irradiation zone under different excitation conditions. Figure 20a presents summary dependences of $^{32}SF_6{}^{32}SF_5^+$ (curves *1* and *1a*) and $^{34}SF_6{}^{32}SF_5^+$ (curves *2* and *2a*) signals on the distance between the nozzle exit and the particle irradiation zone in the case of excitation at the 10P(32) line of the CO_2 laser (frequency 932.96 cm^{-1}), coinciding with the maximum of the low-frequency IR absorption band of $(^{32}SF_6)_2$ dimers [62–64]. The dependences were obtained using an SF_6/Ar mixture with the pressure ratios of 1/80 (curves *1* and *2*) and 1/200

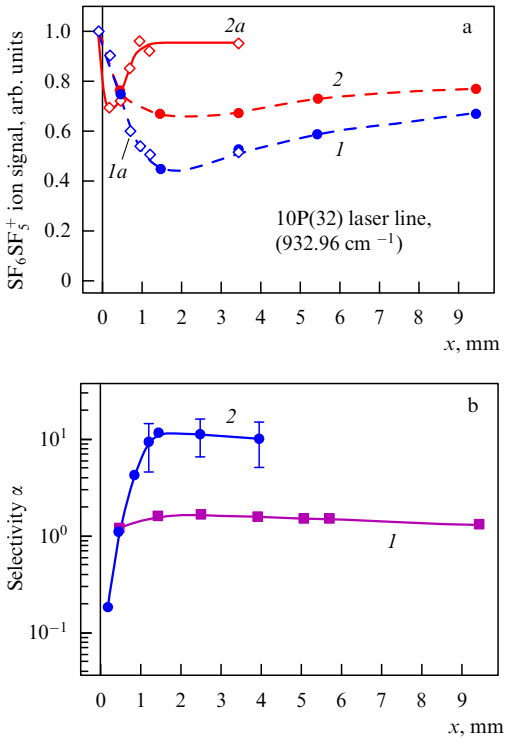

Figure 20. (a) Dependences of $^{32}SF_6{}^{32}SF_5^+$ signals (curves *1* and *1a*) and $^{34}SF_6{}^{32}SF_5^+$ signals (curves *2* and *2a*) on the distance between the irradiation zone and the nozzle. Curves *1* and *2* were obtained using an $SF_6/Ar = 1/80$ mixture, curves *1a* and *2a* using a 1/200 mixture. CO_2 laser power of 4 W, pressure upstream of the nozzle 2 atm [42]. (b) Dependences of selectivity α of cluster dissociation on the distance between nozzle and irradiation zone. Curves *1* and *2* describe 1/80 and 1/200 degrees of dilution, respectively. CO_2 laser power is 4 W, pressure above the nozzle is 2 atm [42].

(curves *1a* and *2a*) at a total gas pressure of 2.0 atm upstream of the nozzle (in all the cases). The data in Fig. 20a are averaged over a large series of measurements. They reveal two characteristic features in the behavior of the obtained dependences that are analyzed separately below.

The first feature is that the $^{32}SF_6{}^{32}SF_5^+$ signal has a maximum value when the laser beam is close to the nozzle exit, whereas the $^{34}SF_6{}^{32}SF_5^+$ signal is minimal (if the mixture is used at a pressure ratio of 1/200), because there are no clusters near the nozzle. Laser radiation at the 10P(32) line interacts with free $^{34}SF_6$ molecules [61], which accounts for the suppression of $^{34}SF_6{}^{32}SF_6$ cluster formation. Further evolution of the signals is related to cluster formation. $(^{32}SF_6)_2$ dimers preferentially interact with radiation at the above laser frequency, whereas $^{34}SF_6{}^{32}SF_6$ dimers are off-resonance with laser radiation [62–64]. Therefore, the $^{34}SF_6{}^{32}SF_5^+$ signals increase in strength with the distance between the nozzle and the particle irradiation zone due to the reduction in the number of free $^{34}SF_6$ molecules in the jet and the absence of resonance between laser radiation and $^{34}SF_6{}^{32}SF_6$ clusters. At the same time, the $^{32}SF_6{}^{32}SF_5^+$ ion signal (curve *1*) weakens with the onset of $^{32}SF_6$ clustering and dissociation of the newly formed $(^{32}SF_6)_2$ dimers. If a 1/80 mixture is used, the positions of minima on curves *1* and *2* roughly correspond to the region of small clusters ($(SF_6)_2$ dimers) and particles like $(SF_6)_2Ar_n$. The further behavior of the observed dependences appears to be determined by the formation and dissociation of larger clusters.

The second peculiarity is related to the essential dependence of cluster dissociation efficiency on the degree of SF_6 dilution in argon. Figure 20a presents the dependences of $^{34}SF_6{}^{32}SF_5^+$ and $^{32}SF_6{}^{32}SF_5^+$ signal values on the distance between the particle excitation zone and the nozzle for two degrees of molecular gas dilution in the carrier gas (argon): $SF_6/Ar = 1/80$ and 1/200. The experimental points for these two degrees of dilution practically coincide in the case of the 'resonant' $^{32}SF_6{}^{32}SF_5^+$ dimer signal (curves *1* and *1a*), but for the depleted off-resonant isotope component $^{34}SF_6{}^{32}SF_5^+$ the behavior of this signal essentially depends on the degree of dilution (curves *2* and *2a*). In the case of low dilution (1/80), curve *2* qualitatively resembles curve *1*. As the degree of dilution increases up to 1/200, the character of distance dependence $^{34}SF_6{}^{32}SF_5^+$ changes radically. The initial growth becomes saturated and the position of the particle irradiation zone does not influence the value of the $^{34}SF_6{}^{32}SF_5^+$ signal up to measurement error. Such a behavior of these dependences appears to be due to the different composition of the newly formed clusters at different dilutions, and therefore, different character of their interaction with radiation. In particular, a high SF_6 dilution in argon can be expected to shift the particle formation process to generate mixed clusters and possibly decrease their internal temperature.

Note that for jet irradiation close to the nozzle exit, when SF_6 molecule clustering is suppressed, selectivity is observed only if the gas under study is highly diluted in the carrier gas (within the 1/100 to 1/200 range) [32–36, 41], because high dilution suppresses inter-isotope vibrational energy exchange between excited and unexcited molecules. Probably, these processes influence the behavior of the dependences presented in Fig. 20a, especially at the starting stage.

The data from Fig. 20a make it possible to determine isotopic selectivity of IR dissociation of $^{32}SF_6{}^{32}SF_6$ clusters with respect to the $^{34}SF_6{}^{32}SF_6$ clusters. Selectivity of cluster dissociation α is defined as the ratio of the losses of dimeric isotope components from the beam:

$$\alpha = \frac{\beta(^{32,32}S)}{\beta(^{34,32}S)}\,, \tag{7.1}$$

$$\beta(^{i,j}S) = 1 - \frac{^{i,j}S}{^{i,j}S_0}\,, \tag{7.2}$$

where $^{32,32}S$, $^{32,32}S_0$, and $^{34,32}S$, $^{34,32}S_0$ are signal values of the respective dimer ion peaks after and before irradiation, respectively. Figure 20b presents the values of selectivity α of the $^{32,32}S$ cluster component with respect to $^{34,32}S$ depending on the distance between the particle irradiation zone and the nozzle for two degrees of gas dilution: $SF_6/Ar = 1/80$ and 1/200 (curves *1* and *2*, respectively). The different behavior of $^{34}SF_6{}^{32}SF_5^+$ and $^{32}SF_6{}^{32}SF_5^+$ signals at different dilutions is responsible for the significant difference between selectivities of cluster dissociation in these two cases (see also Table 3). At the pressure ratio $SF_6/Ar = 1/80$, selectivity remains practically unaltered at the $\alpha \approx 1.7$ level, regardless of the distance between the nozzle and the particle irradiation zone. At the same time, a well apparent growth of selectivity up to $\alpha \approx 15-20$ is observed when the $SF_6/Ar = 1/200$ mixture is used. To recall, the values of $\alpha < 1$ near the nozzle exit correspond to the region where the molecule clustering process is suppressed [37, 38].

Table 3. Some results of selective dissociation of $(SF_6)_m Ar_n$ clusters formed during gas-dynamic expansion of an SF_6/Ar mixture under different experimental conditions [42].

Gas composition and pressure upstream of nozzle, atm	Laser generation line and frequency, cm^{-1}	Laser power, W	Selectivity of mixed cluster dissociation $\alpha(^{32,32}S/^{34,32}S)$	Nozzle pulse duration, ms	Distance x from the particle irradiation zone to the nozzle, mm
SF_6/Ar = 1/200, 1.63	10P(34) — 931.00	4.6	≈ 2	1.2	2
SF_6/Ar = 1/200, 1.63	10P(34) — 931.00	4.6	⩾ 20–25	1.2	7
SF_6/Ar = 1/80, 2.0	10P(32) — 932.96	4	≈ 1.7	1.2	3
SF_6/Ar = 1/200, 2.0	10P(32) — 932.96	4	≈ 15–20	1.2	1.5

7.4 Dependences of IR cluster dissociation on the gas composition and pressure upstream of the nozzle and IR radiation power

Reference [42] reports a study on the influence of gas composition and total pressure upstream of the nozzle and the power of particle-exciting laser radiation on IR dissociation parameters. Some results obtained are presented in Fig. 21. Figure 21a shows dependences of the efficiency and selectivity of $^{32}SF_6{}^{32}SF_6$ and $^{34}SF_6{}^{32}SF_6$ cluster dissociation on the gas pressure in a range of 1.4–2.2 atm when an SF_6/Ar = 1/200 mixture was used. The jet was irradiated at the laser 10P(32) line (frequency 932.96 cm^{-1}) 1.45 mm from the nozzle, i.e., in the region where the molecular clustering process is close to completion (see Fig. 3). It follows from Fig. 21a that the efficacy of cluster dissociation in the case of excitation at a given fixed distance from the nozzle decreases with increasing gas pressure upstream of the nozzle. The causes behind this relationship include lowered temperature, increased size of the clusters forming at an enhanced gas pressure upstream of the nozzle, and changes in cluster composition resulting in a shift of IR absorption bands of the clusters and their going off resonance with laser radiation.

Figure 21b presents the dependences of $^{32}SF_6{}^{32}SF_5^+$ and $^{34}SF_6{}^{32}SF_5^+$ ion signals (curves *1* and *2*, respectively) and the dependences of the degree of beam depletion (losses of the respective $^{32}SF_6{}^{32}SF_6$ and $^{34}SF_6{}^{32}SF_6$ clusters (see (7.1) and (7.2))) (curves *3* and *4*, respectively) on the power of laser radiation exciting particles. Evidently, a rise in the radiation power results in a decrease in $^{32}SF_6{}^{32}SF_5^+$ (curve *1*) and $^{34}SF_6{}^{32}SF_5^+$ (curve *2*) signals, while the respective losses β (curves *3* and *4*) increase. Simultaneously, selectivity falls from $\alpha = 2.07$ at a laser power of 1 W to $\alpha = 1.79$ at 4 W. However, the selectivity decline rate is lower than the growth rate of the cluster dissociation yield. This finding can be of help and importance for the choice of the optimal radiation power in the isotope separation process.

To recall, all measurements of IR dissociation of SF_6 clusters in [42] were made by recording $^{32}SF_6{}^{32}SF_5^+$ and $^{34}SF_6{}^{32}SF_5^+$ dimer ion fragments. It is not unlikely that some contribution to the respective signals came from the ions formed during ionization of larger clusters (including mixed ones) in the QMS chamber. We think, however, that the main contribution to the measured signals was made by $(SF_6)_2$ dimers, especially at the early stages of cluster formation near the nozzle, where the maximum values of selectivity $\alpha \geqslant 10$ were actually obtained.

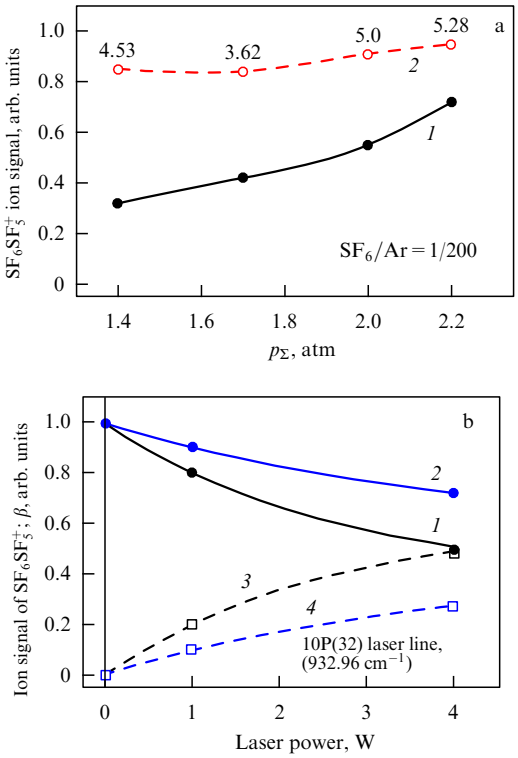

Figure 21. (a) Ion signals versus pressure upstream of the nozzle. Curve *1* — $^{32}SF_6{}^{32}SF_5^+$, curve *2* — $^{34}SF_6{}^{32}SF_5^+$. Numbers indicate selectivity values α. SF_6/Ar = 1/200. (b) Efficiency and selectivity of cluster IR dissociation versus laser radiation power. Curves *1* and *2* — $^{32}SF_6{}^{32}SF_5^+$ and $^{34}SF_6{}^{32}SF_5^+$ signals, respectively, curves *3* and *4* — dependences of beam depletion (losses β) of $^{32}SF_6{}^{32}SF_6$ and $^{34}SF_6{}^{32}SF_6$ clusters (see the text). CO_2 laser is tuned to line 10P(32), distance from the nozzle x = 1.45 mm, dilution SF_6/Ar = 1/80, pressure 2 atm [42].

7.5 Main results and conclusions

The study of isotope-selective dissociation of homogeneous and mixed van der Waals $(SF_6)_m Ar_n$ clusters by IR radiation in [42] gave evidence of the dependence of its effectiveness and selectivity on the frequency and power of exciting laser radiation, gas composition and pressure upstream of the nozzle, and distance between the particle irradiation zone and the nozzle exit section. It also showed that resonant vibrational excitation of the clusters by an IR laser makes possible their isotope-selective dissociation.

It was found that the efficiency of dissociation of the resonant isotope component of the clusters increases and selectivity decreases with the growth of the exciting radiation power. Moreover, the laser radiation frequency markedly affects parameters of isotope-selective IR dissociation of the clusters. Therefore, an adequate choice of the laser radiation frequency is an important prerequisite for the achievement of

optimal efficiency and selectivity of cluster dissociation. This inference is especially important for heavy molecule clusters with a small isotopic shift.

It was shown that relatively high selectivities are realizable in $(SF_6)_m Ar_n$ cluster dissociation. For example, selectivities of $^{32}SF_6{}^{32}SF_6$ cluster dissociation with respect to $^{34}SF_6{}^{32}SF_6$ $\alpha(^{32,32}S/^{34,32}S)$ exceeded 10–20 when an SF_6/Ar mixture at a pressure ratio of 1/200 was used under conditions of jet irradiation at the 10P(32) laser line (frequency 932.96 cm^{-1}). The conditions were found under which optimal selectivity and efficiency of dissociation of homogeneous and mixed $(SF_6)_m Ar_n$ clusters can be reached. Much higher selectivities of dissociation of both homogeneous and mixed molecular clusters than in Refs [33–36] were obtained.

All this information taken together gives a comprehensive view of the processes taking place during IR laser dissociation of molecular clusters having much in common for all other molecules, not only SF_6. The advantages of the proposed method for isotope separation by IR dissociation of the clusters in comparison with the method based on clustering suppression include a much wider range within which particles can be irradiated without marked deterioration of separation parameters. This fact is of special importance in the work with heavy molecules like UF_6.

However, it should be noted that supersonic expansion of a gas at the nozzle exit is, as a rule, accompanied by the formation of numerous clusters of different sizes, which considerably complicated the separation of isotopes by the proposed method. On the other hand, the width of cluster size distribution can be controlled by varying the conditions of gas flow through the nozzle and using optimally-shaped nozzles to ensure the prevalence of dimers in cluster composition. Generally speaking, if the discussion is confined largely to the two approaches (selective suppression of molecule clustering and selective IR dissociation of the clusters), the latter one appears to be the preferable option in certain cases.

8. Isotope-selective IR dissociation of mixed $(CF_3Br)_m Ar_n$ clusters

Isotope-selective IR dissociation of mixed $(CF_3Br)_m Ar_n$ clusters was investigated in Ref. [43] with special reference to the evaluation of the possibility of implementing selective cluster dissociation with respect to bromine isotopes. The studies were carried out using small clusters ($m = 1-2$, $1 \leqslant n \leqslant 5$ are the number of molecules and atoms per cluster, respectively). With the efficiency and selectivity of cluster dissociation depending on gas parameters upstream of the nozzle, the energy and frequency of laser radiation were assessed. It was shown that resonant vibrational excitation of the clusters by IR laser radiation allows their isotope-selective dissociation with respect to bromine isotopes to be realized.

8.1 Substantiation of the method and peculiarities of the experiment

Unlike the $(SF_6)_m Ar_n$ clusters considered in Section 7 and characterized by a relatively large isotopic shift in IR absorption spectra (≈ 17 cm^{-1} for $^{32}SF_6$ and $^{34}SF_6$ molecules [60, 61]), homogeneous and mixed $(CF_3Br)_m Ar_n$ clusters have very small isotopic shifts in their IR absorption and dissociation spectra (≈ 0.245 cm^{-1}) [65]. Moreover, the spectra are markedly broadened due to pre-dissociation [44]. IR dissociation spectra of homogeneous $(CF_3Br)_m$ clusters are ~ 15 cm^{-1} wide (at half-height) [53, 81, 82] and look like virtually structureless bands. As a result, the absorption and dissociation spectra of the clusters containing different CF_3Br isotopomers overlap substantially. This makes practically impossible selective IR dissociation of homogeneous $(CF_3Br)_m$ clusters using lasers.

The situation with small mixed $(CF_3Br)_m Ar_n$ clusters is quite different. The spectra of their IR dissociation have the form of uniformly broadened relatively narrow bands (3.5 cm^{-1} at half-height) [53]. The spectra are localized in the 9.6-μm CO_2 laser generation region of the band (see Figs 23a, b below), making possible, in principle, isotope-selective dissociation (see [43]) at certain laser generation lines at which the maximum difference among the intensities of IR dissociation of the clusters containing different CF_3Br isotopomers is observed.

To choose laser lines at which irradiation is likely to ensure selective cluster dissociation, the authors of [43] analyzed the IR dissociation spectrum of $(CF_3Br)_m Ar_n$ clusters measured from the yield of the $ArBr^+$ ion product in [53]. The analysis allowed estimating the expected selectivity of IR cluster dissociation by irradiation at several CO_2 laser lines in a range from 9R(24) (frequency 1081.087 cm^{-1}) to 9R(30) (1084.625 cm^{-1}) (Table 4). The expected maximum selectivities of the cluster dissociation process at these laser lines proved to be $\alpha(^{79}Br/^{81}Br) = 0.89 \pm 0.06$ and $\alpha(^{79}Br/^{81}Br) = 1.19 \pm 0.07$, respectively.

$(CF_3Br)_m Ar_n$ clusters were generated during gas-dynamic cooling of the mixture of CF_3Br molecules with the carrier gas (Ar) at a pressure ratio of 1/200 as a result of supersonic expansion through the pulsed nozzle having an exit orifice diameter of 0.8 mm. The length of the nozzle opening pulse ranged from 400 to 450 μs (at the half-height), depending on gas pressure and composition upstream of the nozzle. Gas pressure varied from 1.5 to 3 atm. A conical diaphragm with the opening diameter of 3 mm placed 50 mm from the nozzle was used to cut out a cluster beam from the central part of the supersonic flow. The beam thus formed entered the QMS ionization chamber. The distance from the nozzle exit section to the ionization chamber was 250 mm.

In Ref. [43], in contrast with other studies considered in the preceding sections, the clusters were excited by a pulsed CO_2 laser with a pulse energy of 3 J. Laser radiation crossed

Table 4. Results of isotope-selective dissociation of mixed van der Waals $(CF_3Br)_m Ar_n$ clusters at several CO_2 laser radiation lines. The clusters were generated during the gas-dynamic expansion of the CF_3Br/Ar at a pressure ratio of 1/200 and total gas pressure upstream of the nozzle of 3 atm. The presented selectivities were measured at an exciting radiation energy density of 0.04 J cm^{-2} [43].

Laser generation line and frequency, cm^{-1}	Expected selectivity of $\alpha_{exp}(^{79}Br/^{81}Br)$ dissociation	Measured selectivity of $\alpha_{obt}(^{79}Br/^{81}Br)$ dissociation
9R(24) — 1081.087	0.89 ± 0.06	0.95 ± 0.04
9R(26) — 1082.296	1.05 ± 0.05	1.04 ± 0.05
9R(28) — 1083.478	1.18 ± 0.06	1.14 ± 0.06
9R(30) — 1084.635	1.19 ± 0.07	1.16 ± 0.04

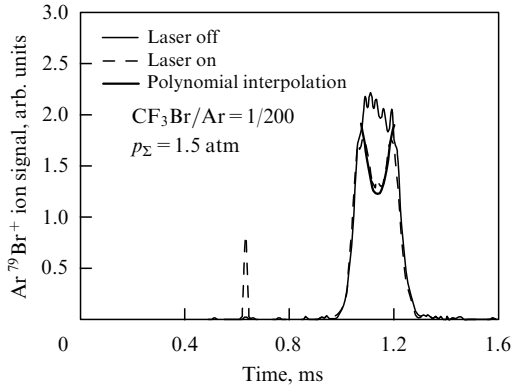

Figure 22. Time dependences of $Ar^{79}Br^+$ ion signals without and with jet laser irradiation at line 9R(28) (frequency1083.48 cm^{-1}) and energy density 0.06 J cm^{-1}. The pressure of $CF_3Br/Ar = 1/200$ mixture upstream of the nozzle is 1.5 atm. The peak shown by the dashed curve on the left results from electrical inducing by a laser pulse.

the molecular cluster beam at an angle of approximately 90°. To increase the irradiated beam volume, radiation that passed through the chamber was reflected back at a small angle to the previous one. As a result, about a third of the pulsed cluster beam was irradiated (Fig. 22). The size of the IR radiation spot at the intersection with the cluster beam averaged over two passages amounted to 7.8×32 mm. The nozzle was 1.7 cm apart from the center of the particle irradiation zone. Clustering was completed for the particle flight time to this zone [37–42].

8.2 Measurement procedure

The experiments reported in [43] were designed to measure $Ar^{79}Br^+$ and $Ar^{81}Br^+$ ion signals from $(CF_3Br)_mAr_n$ mixed clusters without beam irradiation and with its irradiation by a laser. The measured ion mass peaks of $Ar^{79}Br^+$ and $Ar^{81}Br^+$ fragments were approximated by Gaussian functions. Isotopic selectivity of dissociation of the clusters containing the ^{79}Br isotope with respect to the clusters containing ^{81}Br was determined as

$$\alpha\left(\frac{^{79}Br}{^{81}Br}\right) = \frac{\beta_{79}}{\beta_{81}}\,, \tag{8.1}$$

where β_{79} and β_{81} are $CF_3{}^{79}Br$-Ar and $CF_3{}^{81}Br$-Ar dissociation yields in the laser-irradiated jet volume. The yields of dissociation in the irradiated beam volume were found from the relations

$$S_{1L} = S_{10}(1 - \beta_{79})\,, \tag{8.2}$$

$$S_{2L} = S_{20}(1 - \beta_{81})\,, \tag{8.3}$$

where S_{1L} and S_{2L} are the areas under the Gaussian curves for $Ar^{79}Br^+$ and $Ar^{81}Br^+$ ion signals, respectively, in the case of beam irradiation, and S_{10} and S_{20} are the areas under the Gaussian curves for $Ar^{79}Br^+$ and $Ar^{81}Br^+$ ion signals in the absence of irradiation.

The use of (8.1)–(8.3) yields the final formula for calculating isotopic selectivity of cluster dissociation:

$$\alpha\left(\frac{^{79}Br}{^{81}Br}\right) = \frac{1 - S_{1L}/S_{10}}{1 - S_{2L}/S_{20}}\,. \tag{8.4}$$

Factors of cluster beam enrichment with ^{79}Br and depletion of this isotope were calculated from the formula

$$K_{enr}(^{79}Br) = \frac{S_{1L}/S_{2L}}{S_{10}/S_{20}}\,. \tag{8.5}$$

Synchronization of laser radiation and molecular beam pulses was monitored based on the temporal position of the 'dip-burning' amplitude maximum in the $Ar^{79}Br^+$ signal (see Fig. 22).

8.3 Results of research and their analysis

It was mentioned in Section 6.2 that the generation of mixed $(CF_3Br)_mAr_n$ clusters requires strong cooling of the particles in an expanding jet [78, 83]. The jet temperature needed for the formation of $(CF_3Br)_mAr_n$ mixed clusters must be significantly lower than for the generation of homogeneous $(CF_3Br)_m$ clusters [83]. With this in mind, the authors of [43] used a highly diluted mixture of CF_3Br gas in argon (CF_3Br/Ar) with the pressure ratio of 1/200 and total gas pressure upstream of the nozzle of 1.5 and 3 atm.

These conditions favored the effective formation of mixed clusters containing a small number ($m = 1-2$) of CF_3Br molecules and a few ($n = 1-5$) argon atoms [78]. At the same time, the probability of generating large homogeneous $(CF_3Br)_m$ clusters was questionable [78]. The use of a low total gas pressure upstream of the nozzle and a strongly diluted mixture facilitated the generation of small heterogeneous clusters and improved separation by cluster dissociation [43].

Figure 22 demonstrates the time dependence (time-of-flight spectrum) of the $Ar^{79}Br^+$ the ion signal in the absence of cluster beam irradiation (curve *1*) and in the case of its irradiation by a laser pulse at the 9R(28) line (frequency 1083.48 cm^{-1}) at an energy density of exciting radiation 0.06 J cm^{-2} (curve *2*). The total gas pressure upstream of the nozzle is 1.5 atm. Clearly, beam irradiation by a laser pulse results in 'burning out' the dip in the time dependence of the $Ar^{79}Br^+$ cluster ion signal. The depth of the dip equaling the cluster dissociation yield depends on the exciting radiation energy density, determined from relation (8.2). Dip width and position allow the part of the cluster beam irradiated by the laser to be identified.

The dependences of the dissociation yield β_{79} of $CF_3{}^{79}Br$-Ar clusters on exciting IR radiation energy density Φ_{IR} were measured (by the $Ar^{79}Br^+$ ion cluster signal) in [43] for a few laser generation lines coinciding in frequency with the IR dissociation spectrum of mixed clusters. $\beta_{79}(\Phi_{IR})$ dependences were used to obtain spectral dependences of the IR dissociation yield $\beta_{79}(\nu)$ of $CF_3{}^{79}Br$-Ar clusters at different exciting radiation energy densities. One such dependence at energy density $\Phi_{IR} = 0.008$ J cm^{-2} is presented in Fig. 23a. For comparison, Fig. 23a shows also the spectral dependence of the $Ar^{79}Br^+$ signal from [53]. Evidently, the spectral dependence of the cluster dissociation yield in [43] is in excellent agreement with that in [53]. It was concluded based on the dependence $\beta_{79}(\nu)$ that isotope-selective cluster dissociation is possible at certain laser generation lines.

Selectivity of $(CF_3Br)_mAr_n$ cluster dissociation was documented in [43] based on measurements of the mass spectra of $Ar^{79}Br^+$, Ar_3^+, and $Ar^{81}Br^+$ cluster fragments ($m/z = 119$, 120, and 121 amu) in the absence of beam irradiation and with its irradiation by a CO_2 laser as

described in Section 6.2 and shown in Figs 16a, b. For example, irradiation of the clusters at the 9R(28) laser line (frequency of 1083.48 cm^{-1}) and energy density of 0.054 J cm^{-2} (total gas pressure upstream of the nozzle of 3 atm) produced the enrichment factor $K_{enr}(^{79}Br) = 0.88$, with selectivity of the cluster dissociation process being $\alpha(^{79}Br/^{81}Br) = 1.15$ [43].

Figure 23b shows frequency dependences of selectivity $\alpha(^{79}Br/^{81}Br)$ of $(CF_3Br)_mAr_n$ cluster dissociation at two exciting radiation energy densities: 0.04 and 0.08 J cm^{-2}. It can be seen that slightly higher selectivity is observed at lower energy densities, probably because of a transition to the linear cluster excitation regime. Selectivity was close to unity at the 9R(26) line near which the maximum of the cluster IR dissociation spectrum was localized and the differences among the intensities of the spectra of the clusters containing different CF_3Br isotopomers was minimal (see also Table 4). Maximum selectivity was observed at the wings of the cluster IR dissociation spectrum where the spectral dependence gradient of the $ArBr^+$ ion yield is large. Selectivity $\alpha(^{79}Br/^{81}Br)$ dissociation was lower than unity at the 9R(24) line frequency and higher than that at the 9R(30) line which corresponds to the frequency position of cluster IR dissociation spectra. In other words, these experiments confirmed the possibility of cluster beam enrichment with (or depletion in) any of the bromine isotopes [43].

8.4 Conclusions

The main objective of Ref. [43] was to elucidate the possibility of selective dissociation of mixed $(CF_3Br)_mAr_n$ clusters with respect to bromine isotopes using a CO_2 laser. The data obtained appear to demonstrate such a possibility. At the same time, there are a large number of unknown characteristics and parameters of the proposed method, such as cluster temperature and concentration in the region of their interaction with laser radiation, cluster size distribution, the width of IR absorption spectra, and dissociation spectra of specifically sized clusters. Optimization and consideration of all these factors are indispensable if high enrichment coefficients and selectivity of the IR cluster dissociation process are to be obtained.

It was shown in [43] that the use of CO_2 laser radiation for the resonant vibrational excitation of $(CF_3Br)_mAr_n$ clusters makes possible their selective dissociation with respect to bromine isotopes. For example, the use of a CF_3Br/Ar mixture at a pressure ratio of 1/200 allowed obtaining factors of enrichment with the ^{79}Br isotope $K_{enr}(^{79}Br) = 1.15 \pm 0.04$ and $K_{enr}(^{79}Br) = 0.95 \pm 0.03$ under conditions of cluster irradiation at the 9R(30) ($\nu = 1084.635$ cm^{-1}) and 9R(24) ($\nu = 1081.087$ cm^{-1}) lines. The selectivities of cluster dissociation thus achieved amount to 1.16 ± 0.05 and 0.95 ± 0.04, respectively. These results give reason to believe that the proposed method can be employed to separate isotopes of heavy elements in molecules with a slight isotopic shift in IR absorption spectra.

Isotope-selective suppression of the clustering of molecules among themselves and with argon atoms can be used in principle to design the isotope separation process. One of the conceivable variants of its implementation includes two stages. First is selective suppression of the clustering of a chosen isotopic modification of the molecules leading to their distribution in the beam at a larger solid angle than that of the distribution of colder and heavier clusters containing nontarget molecules. Second is the spatial separation of target

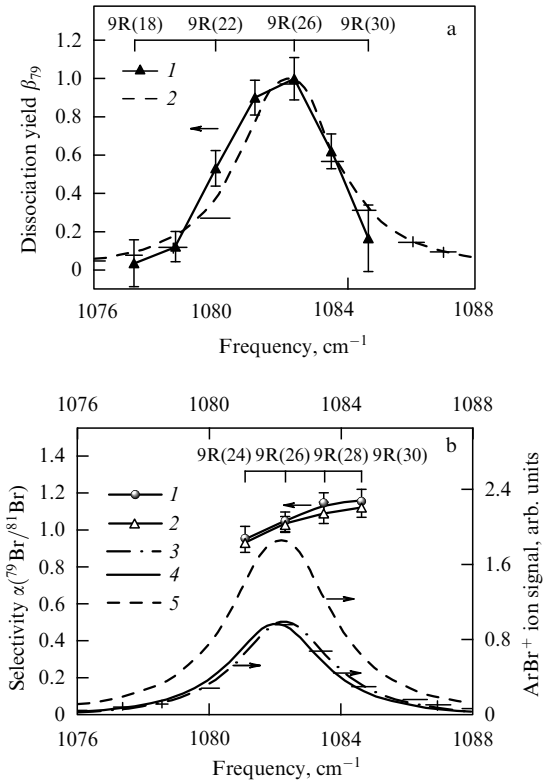

Figure 23. (a) Frequency dependences of (*1*) $(CF_3Br)_mAr_n$ cluster dissociation yield at excitation energy density $\Phi_{IR} = 0.008$ J cm^{-2} and $CF_3Br/Ar = 1/200$ mixture pressure upstream of the nozzle of 1.5 atm; (*2*) $ArBr^+$ ion signal from [53]. (b) Dependences of $(CF_3Br)_mAr_n$ cluster dissociation selectivity on the exciting laser radiation frequency at energy densities (*1*) 0.04 J cm^{-2} and (*2*) 0.08 J cm^{-2}; $CF_3Br/Ar = 1/200$ mixture pressure upstream of the nozzle of 3 atm. Frequency dependences of (*3*) $Ar^{79}Br^+$, (*4*) $Ar^{81}Br^+$ ion signals, and (*5*) integral $ArBr^+$ ion signal from [53]. (Taken from [43].)

molecules from the cluster beam. Such a scheme for the achievement of the maximum separation coefficient requires not only high optical selectivity of IR excitation of the necessary isotopic modifications of the molecules but also a high enough selectivity during the spatial separation of target molecules from the cluster beam.

9. Conclusions

The foregoing detailed research work on laser-assisted isotope separation was carried out with the use of low-energy methods of MLIS, including isotope-selective suppression of molecule clustering during gas-dynamic expansion at the nozzle exit and isotope-selective IR dissociation of van der Waals clusters. The dependences of the main parameters of the isotope separation process (efficiency and selectivity) on characteristics of exciting laser radiation (frequency and power), gas composition and pressure upstream of the nozzle, and distance between the particle irradiation zone and the nozzle exit were obtained. The conditions are formulated for the achievement of high selectivity and efficiency of the isotope separation process.

Experiments with SF_6 molecules using both isotope-selective suppression of molecule clustering and isotope-selective IR dissociation of clusters demonstrated higher enrichment and selectivity coefficients than those reported in earlier publications [32–36].

It was shown that rather high selectivity can be reached by suppressing the clustering of SF_6 molecules among themselves and with argon atoms. Dissociation of homogeneous and mixed $(SF_6)_m Ar_n$ clusters proved equally efficient. For example, the use of the SF_6/Ar mixture at a pressure ratio of 1/200 allowed reaching a selectivity of $^{32}SF_6{}^{32}SF_6$ cluster dissociation with respect to $^{34}SF_6{}^{32}SF_6$ clusters $\alpha(^{32,32}S/^{34,32}S) \geqslant 10-20$ under conditions of particle irradiation at the 10P(32) laser line (frequency 932.96 cm^{-1}). Control of SF_6 molecule clustering with argon atoms ensured a very high selectivity $\alpha(^{32}SF_6/^{34}SF_6) \geqslant 25-30$ when the particles were irradiated at the 10P(16) laser line (frequency 947.74 cm^{-1}).

Experiments with CF_3Br molecules provided data on selective suppression of molecule clustering among themselves and with argon atoms that give evidence of the possibility of controlling molecule clustering selective with respect to bromine isotopes and thereby realizing isotope separation by this method with a very small isotopic shift (≈ 0.25 cm^{-1}) in the excited molecule vibration characteristic of UF_6.

Isotope-selective IR dissociation of mixed $(CF_3Br)_m Ar_n$ clusters characterized by a slight isotopic shift in the spectra ($\leqslant 0.25$ cm^{-1}) has been realized. It was shown that isotope-selective dissociation of the clusters is possible, despite small isotopic shifts, if they have relatively narrow dissociation spectra ($\leqslant 2-3$ cm^{-1} at half-height). The selectivity of dissociation $\alpha(^{79}Br/^{81}Br)$ during $(CF_3Br)_m Ar_n$ irradiation at the laser 9R(30) line (frequency 1084 cm^{-1}) was estimated at 1.16.

Comparing the data on isotope-selective suppression of molecule clustering and isotope-selective IR dissociation of the clusters indicates that the latter approach is sometimes preferable to the former if high efficiency and selectivity are to be achieved. It allows easy realization of irradiation of a large part of a molecular cluster beam.

Both methods are currently regarded as the most promising ones. According to Silex Systems Ltd, Australia [1, 22, 23], the efficiency of enrichment using the SILEX technology is much higher (by a factor of 1.6–16) than that using modern centrifugal techniques. Nevertheless, the analysis shows [31] that the efficiency (productivity) of both methods is relatively low, the cause being the necessity to use highly diluted molecular mixtures in a carrier gas. The method of suppression of molecule clustering is characterized by a very small region within which the effect of selective control over molecule clustering is localized. The efficiency of isotope-selective IR dissociation is limited due to the formation of a variety of differently sized clusters in molecular beams. This not only worsens selectivity of the isotope separation process but also makes very difficult its realization by this technique. Hence, the importance of the detailed evaluation of the method proposed and implemented in Refs [28–31] (see also review [1]) for isotope-selective IR dissociation of molecules under the nonequilibrium thermodynamic conditions of a compression shock forming in front of the hard surface onto which an intense pulsed molecular flow is incident.

To conclude, the methods considered in this review and the results of their application are of great importance not only in the context of the development of laser-aided techniques for isotope separation but also in terms of investigation into the process of cluster fragmentation by IR laser radiation [44] and control of both parameters and composition of molecular cluster beams [56].

The author is grateful to V M Apatin, V N Lokhman, A L Malinovskii, N-D D Ogurok, A N Petin, D G Poidashev, and E A Ryabov for their collaboration and instructive discussions. Special thanks are due to A N Petin for his expert handling of drawings. The work was supported in part by the Russian Foundation for Basic Research (grant 18-02-00242).

References

1. Makarov G N *Phys. Usp.* **58** 670 (2015); *Usp. Fiz. Nauk* **185** 717 (2015)
2. Eerkens J W *Nucl. Sci. Eng.* **150** 1 (2005)
3. Eerkens J W *Laser Part. Beams* **23** 225 (2005)
4. Makarov G N, Petin A N *JETP* **103** 697 (2006); *Zh. Eksp. Teor. Fiz.* **130** 804 (2006)
5. Makarov G N *Phys. Usp.* **49** 1131 (2006); *Usp. Fiz. Nauk* **176** 1155 (2006)
6. Kim J, Eerkens J W, Miller W H *Nucl. Sci. Eng.* **156** 219 (2007)
7. Kim J et al. "Current «status of the MLIS uranium enrichment process", in *Transactions of the Korean Nuclear Society Spring Meeting. Jeju, Korea, May 22, 2009*, p. 455
8. Eerkens J W, Kim J *AIChE J.* **56** 2331 (2010)
9. Makarov G N, Petin A N *JETP Lett.* **93** 109 (2011); *Pis'ma Zh. Eksp. Teor. Fiz.* **93** 123 (2011)
10. Lyakhov K A, Lee H J *Appl. Phys. B* **111** 261 (2013)
11. Makarov G N, Petin A N *JETP* **119** 398 (2014); *Zh. Eksp. Teor. Fiz.* **146** 455 (2014)
12. Lyakhov K A, Lee H J *J. Laser Appl.* **27** 022008 (2015)
13. Lyakhov K A, Lee H J, Pechen A N *Separat. Purificat. Technol.* **176** 402 (2017)
14. Bagratashvili V N et al. *Multiple Photon Infrared Laser Photophysics and Photochemistry* (Chur: Harwood Acad. Publ., 1985)
15. Cantrell C D (Ed.) *Multiple-Photon Excitation and Dissociation of Polyatomic Molecules* (Topics in Current Physics, Vol. 35) (Berlin: Springer-Verlag, 1986)
16. Lyman J L, in *Laser Spectroscopy and Its Applications* (Optical Engineering, Vol. 11, Eds L J Radziemski, R W Solarz, J A Raisner) (New York: M. Dekker, 1987) p. 417
17. Makarov G N *Phys. Usp.* **48** 37 (2005); *Usp. Fiz. Nauk* **175** 41 (2005)
18. Baranov V Yu et al., in *Fiziko-khimicheskie Protsessy pri Selektsii Atomov i Molekul. Sbornik Dokladov 2-i Vseross. Nauchnoi Konf., g. Zvenigorod, 1997* (Physico-Chemical Processes in the Selection of Atoms and Molecules. Proc. of the 2nd All-Russian Scientific Conf., Zvenigorod, 1997) (Eds V Yu Baranov, Yu A Kolesnikov) (Moscow: TsNIIatominform, 1997) p. 21
19. Letokhov V S, Ryabov E A, in *Izotopy: Svoistva, Poluchenie, Primenenie* (Isotopes: Properties, Production, Application) (Ed. V Yu Baranov) (Moscow: IzdAT, 2000) p. 329
20. Baranov V Yu, Dyad'kin A P, in *Izotopy: Svoistva, Poluchenie, Primenenie* (Isotopes: Properties, Production, Application) (Ed. V Yu Baranov) (Moscow: IzdAT, 2000) p. 343
21. Letokhov V S, Ryabov E A, in *The Optics Encyclopedia. Basic Foundations and Practical Applications* Vol. 2 (G-L) (Eds Th G Brown et al.) (New York: Wiley-VCH, 2004) pp. 1015–1028
22. SILEX Systems Limited, http://www.silex.com.au
23. SILEX Process, http://www.chemeurope.com/en/encyclopedia/Silex_Process.html
24. SILEX Uranium Enrichment, SILEX Annual Report 2014, http://www.silex.com.au/Silex/media/Announcements/18-SLX-Annual-Report-2014_1.pdf?ext=.pdf
25. SILEX Uranium Enrichment, SILEX Annual Report 2017, http://www.silex.com.au/Silex/media/Corporate-Governance/7-SLX-Annual-Report-2017-270917_1.pdf?ext=.pdf
26. SILEX Uranium Enrichment, SILEX Annual Report 2018, http://www.silex.com.au/Silex/media/Corporate-Governance/10-SLX-Annual-Report-2018-081018_2.pdf?ext=.pdf
27. Lyman J L "Enrichment separative capacity for SILEX", Report LA-UR-05-3786 (Los Alamos, NM: Los Alamos National Laboratory, 2005)
28. Makarov G N, Petin A N *Chem. Phys. Lett.* **323** 345 (2000)
29. Makarov G N, Petin A N *Chem. Phys.* **266** 125 (2001)

30. Makarov G N *Phys. Usp.* **46** 889 (2003); *Usp. Fiz. Nauk* **173** 913 (2003)
31. Makarov G N, Petin A N *Quantum Electron.* **46** 248 (2016); *Kvantovaya Elektron.* **46** 248 (2016)
32. Zellweger J-M et al. *Phys. Rev. Lett.* **52** 522 (1984)
33. Philippoz J-M et al. *J. Phys. Chem.* **88** 3936 (1984)
34. Philippoz J-M et al. *Surf. Sci.* **156** 701 (1985)
35. Philippoz J-M et al. *Ber. Bunseng. Phys. Chem.* **89** 291 (1985)
36. Van den Bergh H *Laser Optoelectron.* (3) 263 (1985)
37. Apatin V M et al. *JETP* **125** 531 (2017); *Zh. Eksp. Teor. Fiz.* **152** 627 (2017)
38. Apatin V M et al. *Quantum Electron.* **48** 157 (2018); *Kvantovaya Elektron.* **48** 157 (2018)
39. Apatin V M et al. *JETP* **127** 244 (2018); *Zh. Eksp. Teor. Fiz.* **154** 287 (2018)
40. Makarov G N, Ogurok N-D D, Petin A N *Quantum Electron.* **48** 667 (2018); *Kvantovaya Elektron.* **48** 667 (2018)
41. Lokhman V N et al. *Laser Phys.* **28** 105703 (2018)
42. Lokhman V N et al. *JETP* **128** 188 (2019); *Zh. Eksp. Teor. Fiz.* **155** 216 (2019)
43. Petin A N, Makarov G N *Quantum Electron.* **49** 593 (2019); *Kvantovaya Elektron.* **49** 593 (2019)
44. Makarov G N *Phys. Usp.* **60** 227 (2017); *Usp. Fiz. Nauk* **187** 241 (2017)
45. Kappes M, Leutwyler S, in *Atomic and Molecular Beam Methods* Vol. 1 (Ed. G Scoles) (New York: Oxford Univ. Press, 1988) p. 380
46. Lee Y T "Isotope separation by photodissociation of Van der Waals molecules"", US Patent 4,032,306 (1977)
47. Lisy J M et al. "Infrared vibrational predissociation spectroscopy of small molecular clusters", in *Laser Spectroscopy V* (Springer Series in Optical Sciences, Vol. 30, Eds A R W McKellar, T Oka, B P Stoicheff) (Berlin: Springer, 1981) p. 324; Report LBL-12981 (Berkeley, CA: Lawrence Berkeley Laboratory, 1981)
48. Casassa M P et al. *J. Chem. Phys.* **72** 6805 (1980)
49. Casassa M P, Bomse D S, Janda K C *J. Chem. Phys.* **74** 5044 (1981)
50. Casassa M P, Bomse D S, Janda K C *J. Phys. Chem.* **85** 2623 (1981)
51. Okada Y et al. *J. Mol. Struct.* **410–411** 299 (1997)
52. Janda K C *Adv. Chem. Phys.* **60** 201 (1985)
53. Celii F G, Janda K C *Chem. Rev.* **86** 507 (1986)
54. Miller R E *J. Phys. Chem.* **90** 3301 (1986)
55. Buck U *Adv. At. Mol. Opt. Phys.* **35** 121 (1995)
56. Makarov G N *Phys. Usp.* **61** 617 (2018); *Usp. Fiz. Nauk* **188** 689 (2018)
57. Pine A S, Robiette A G *J. Mol. Spectr*osc. **80** 388 (1980)
58. Patterson C W, Krohn B J, Pine A S *Opt. Lett.* **6** 39 (1981)
59. Patterson C W, Krohn B J, Pine A S *J. Mol. Spectrosc.* **88** 133 (1981)
60. McDowell R S et al. *Spectrochim. Acta A* **42** 351 (1986)
61. Baldacchini G, Marchetti S, Montelatici V *J. Mol. Spectrosc.* **91** 80 (1982)
62. Geraedts J et al. *Chem. Phys. Lett.* **78** 277 (1981)
63. Geraedts J, Stolte S, Reuss J *Z. Phys. A* **304** 167 (1982)
64. Geraedts J et al. *Faraday Discuss. Chem. Soc.* **73** 375 (1982)
65. Pietropolli Charmet A et al. *Phys. Chem. Chem. Phys.* **8** 2491 (2006)
66. Baranov V Yu et.al. "Lazerno-molekulyarnoe razdelenie izotopov urana" ("Laser-molecular separation of uranium isotopes"), in *Izotopy*: *Svoistva, Poluchenie, Primenenie* (Isotopes: Properties, Production, Application) Vol. 1 (Ed. V Yu Baranov) (Moscow: Fizmatlit, 2005) p. 474
67. Bagratashvili V N et al. *Sov. Phys. JETP* **50** 1075 (1979); *Zh. Eksp. Teor. Fiz.* **77** 2238 (1979)
68. Makarov G N et al. *Quantum Electron.* **28** 530 (1998); *Kvantovaya Elektron.* **25** 545 (1998)
69. Lokhman V N, Ogurok D D, Ryabov E A *Chem. Phys.* **333** 85 (2007)
70. Lokhman V N, Ogurok D D, Ryabov E A *JETP* **108** 727 (2009); *Zh. Eksp. Teor. Fiz.* **135** 835 (2009)
71. Lokhman V N, Ogurok D D, Ryabov E A *Eur. Phys. J. D* **67** 66 (2013)
72. Apatin V M et al. *JETP Lett.* **97** 697 (2013); *Pis'ma Zh. Eksp. Teor. Fiz.* **97** 800 (2013)
73. Apatin V M et al. *Laser Phys. Lett.* **12** 016002 (2015)
74. Apatin V M et al. *JETP* **120** 191 (2015); *Zh. Eksp. Teor. Fiz.* **147** 218 (2015)
75. Avatkov O N et al. *Sov. J. Quantum Electron.* **15** 375 (1985); *Kvantovaya Elektron.* **12** 576 (1985)
76. Takahashi M et al. *Appl. Phys. B* **41** 91 (1986)
77. Melinon P et al. *Chem. Phys.* **84** 345 (1984)
78. Apatin V M et al. *JETP Lett.* **104** 425 (2016); *Pis'ma Zh. Eksp. Teor. Fiz.* **104** 440 (2016)
79. Takeuchi K et al. *J. Nucl. Sci. Technol.* **26** 301 (1989)
80. Jensen R J et al. *Laser Focus* **12** (5) 51 (1976)
81. Geraedts J et al. *Chem. Phys. Lett.* **106** 377 (1984)
82. Liedenbaum C et al. *Z. Phys. D* **11** 175 (1988)
83. Makarov G N *Phys. Usp.* **53** 179 (2010); *Usp. Fiz. Nauk* **180** 185 (2010)